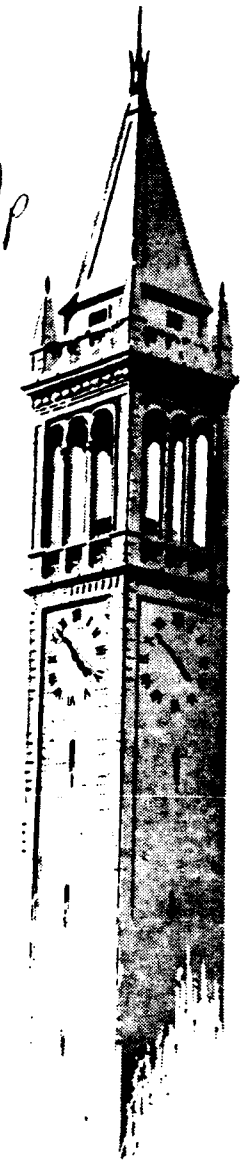



# RADIATIVE ENERGY TRANSFER TO OUTER BASE REGIONS OF CYLINDRICAL AND CONICAL GAS BODIES

by

C. L. Tien and
M. M. Abu-Romia



(NASA Report No. AS-63-4
Contract NAS8-850)
October 24, 1963

Aeronautical Sciences Lab.
INSTITUTE OF ENGINEERING RESEARCH
05197S1
UNIVERSITY OF CALIFORNIA
Berkeley, California

CONTRACT NO. NAS 8-850
REPORT NO. AS-63-4
OCTOBER 24, 1963

SPONSORED BY
THE GEORGE C. MARSHALL SPACE FLIGHT CENTER
NATIONAL AERONAUTICS & SPACE ADMINISTRATION
HUNTSVILLE, ALABAMA

# RADIATIVE ENERGY TRANSFER TO OUTER BASE REGIONS OF CYLINDRICAL AND CONICAL GAS BODIES

by

C. L. Tien

M. M. Abu-Romia

University of California at Berkeley
Aeronautical Sciences Laboratory



FACULTY INVESTIGATORS:

W. H. GIEDT, Professor of Aeronautical Sciences
C. L. TIEN, Assistant Professor of Mechanical Engineering

16710

## SUMMARY

A

The radiative energy transfer to the base regions of a rocket from exhaust plumes is studied analytically by considering the radiation from semi-infinite cylindrical and infinite conical gas bodies of uniform temperature and composition. The effect of nozzle shielding is considered. The results are in terms of the local apparent emissivity in the base region. The expression for the spectral apparent emissivity is in the integral form and requires in general a numerical integration. For semi-infinite cylindrical gas bodies of small absorption coefficient, two asymptotic formulas obtained by direct integration are given. Numerical results are presented for the spectral apparent emissivity as a function of the cone angle which is zero for a cylinder, the height of shielding, the spectral absorption coefficient, and the radial distance in the base plane from the gas body. An approximate method for calculating the total apparent emissivity with any given infrared absorption spectrum of the gas is suggested by utilizing the concept of mean path length. The method is illustrated by the calculation of the total apparent emissivity for semi-infinite cylindrical gas bodies of $CO_2$ and $H_2O$ at high temperatures.

AUTHOR

TABLE OF CONTENTS

## NOMENCLATURE

| | |
|---|---|
| $a$ | effective absorption coefficient based on gray-gas assumption, 1/ft. |
| $a_\lambda$ | spectral absorption coefficient, 1/ft. |
| $A$ | dimensionless effective absorption coefficient ($A = a\ r_e$) |
| $A_\lambda$ | dimensionless spectral absorption coefficient ($A_\lambda = a_\lambda\ r_e$) |
| $b$ | characteristic length defined by Eq. (C-6), ft. |
| $B$ | parameter defined by Eq. (53), dimensionless |
| $c$ | characteristic length defined by Eq. (C-1), ft. |
| $c_1$ | first constant of Planck's law of radiation, $ft^2$Btu/hr |
| $c_2$ | second constant of Planck's law of radiation, ft °R |
| $C$ | parameter defined by Eq. (50), dimensionless |
| $d$ | characteristic length defined by Eq. (C-3), ft. |
| $D_{ni}$ | relative cumulative spectral radiance of a black body, defined by Eq. (18), dimensionless |
| $e$ | characteristic length defined by Eq. (C-5), ft. |
| $E_1$ | elliptic integral of the first kind defined by Eq. (A-14), dimensionless |
| $E_2$ | elliptic integral of the second kind defined by Eq. (A-15), dimensionless |
| $E_{b\lambda}$ | spectral black-body emissive power, Btu/hr $ft^2$ micron |
| $F$ | configuration factor, dimensionless |
| $F_1$ | configuration factor for the tangent region of a conical gas body, dimensionless |
| $F_{11}$ | first partial configuration factor defined by Eq. (E-3), dimensionless |
| $F_{12}$ | second partial configuration factor defined by Eq. (E-4), dimensionless |

$F_{13}$ third partial configuration factor defined by Eq. (E-6), dimensionless

$F_2$ configuration factor for the asymptote region of a conical gas body, dimensionless

h height of the shielded portion of the gas body measured from the base plane, ft.

H dimensionless height of shielding ($H = h/r_e$), dimensionless

$\overline{H}$ dimensionless axial distance measured from the base plane, due to shielding, shown in Fig. 10, dimensionless

i characteristic length defined by Eq. (C-2), ft.

$I_{b\lambda}$ spectral black-body intensity, Btu/hr sq ft steradian

j characteristic length defined by Eq. (C-1), ft.

K parameter defined as $K = 1/R$ in Eqs. (A-14) and (A-15), dimensionless

L dimensionless mean path length

$L_1$ characteristic length defined by Eq. (C-8), ft.

$L_2$ characteristic length defined by Eq. (C-9), ft.

m parameter defined by Eq. (A-4), dimensionless

M parameter defined by Eq. (56), dimensionless

N parameter defined by Eq. (29), dimensionless

P parameter defined by Eq. (29), dimensionless

$P_o$ value of parameter P evaluated at $\beta_o$, defined by Eq. (32), dimensionless

$Q_\lambda$ spectral radiative energy flux, Btu/hr $ft^2$

r radial distance, ft.

$r_e$ bottom radius of the unshielded portion of gas body, ft.

$r_o$ distance measured from viewed plane, ft.

R dimensionless radial distance ($R = r/r_e$), dimensionless

$R_o$ dimensionless distance measured from viewed plane ($R_o = r_o/r_e$), dimensionless

s path length through gas body, ft.

s' projection of the path length on the horizontal plane, ft.

S dimensionless path length ($S = s/r_e$), dimensionless

T absolute temperature, °R.

x distance measured from viewed plane axis, ft.

X dimensionless distance from viewed plane ($X = x/r_e$), shown in Fig. 10, dimensionless

y distance along viewed plane axis measured from vertex of cone, ft.

Y dimensionless distance along viewed plane axis ($Y = y/r_e$) measured from vertex of cone, shown in Fig. 10, dimensionless

$Y_o$ dimensionless distance along viewed plane, measured from the vertex to the point corresponding to $\beta'_o$, dimensionless

Greek Letters

$\alpha$ one-half apex angle of cone, radian

$\beta$ polar angle, radian

$\beta'$ projection of polar angle onto vertical plane, radian

$\beta'_1$ upper limiting angle, due to shielding, given by Eq. (D-4) for cone, radian

$\beta_2'$ lower limiting angle, due to shielding, given by Eq. (D-1) for cone, radian

$\beta_o'$ limit of integration on $\beta'$ defined by Eqs. (23) and (42) for cylindrical and conical gas bodies, respectively, radian

$\beta_c'$ critical angle on $\beta'$ defined by Eq (41), radian

$\epsilon$ total apparent emissivity, dimensionless

$\epsilon_\lambda$ spectral apparent emissivity, dimensionless

$\epsilon_{\lambda c}$ parameter defined by Eqs. (7) and (9), dimensionless

$\epsilon_{\lambda c_1}$ partial effect of the tangent region of cone on $\epsilon_{\lambda c}$ defined by the first integral in Eq. (60), dimensionless

$\epsilon_{\lambda c_2}$ partial effect of the asymptote region of cone on $\epsilon_{\lambda c}$ defined by the second integral in Eq. (60), dimensionless

$\eta$ parameter defined by Eq. (A-1), dimensionless

$\eta_o$ value of the parameter $\eta$ evaluated at $\beta_o'$, defined by Eq. (A-3), dimensionless

$\theta$ inclination of the viewed plane to the cone axis, defined by Eq. (43), radian

$\lambda$ wavelength of radiation, micron

$\lambda_{1i}$ lower limit on wavelength for band absorption i, micron

$\lambda_{2i}$ upper limit on wavelength for band absorption i, micron

$\sigma$ Stefan-Boltzmann constant, Btu/hr $ft^2$ $R^4$

$\tau$ limit of integration on the elliptic integrals in Eqs. (A-14) and (A-15), radian

$\varphi$ azimuth angle, radian

$\varphi_o$ limit of integration on $\varphi$ defined by Eq. (22), radian

$\varphi_{ot}$ limit of integration on $\varphi$ in the tangent region, defined by Eq. (39), radian

$\varphi_{oa}$ limit of integration on $\varphi$ in the asymptote region, defined by Eq. (40), radian

$\Phi$ Schmidt function defined by Eq. (33), dimensionless

$\Psi$ variable of integration introduced in Eqs. (A-14) and (A-15), radian

LIST OF FIGURES

# INTRODUCTION

In the design of large booster vehicles it is recognized that the base regions should be protected against heating by the rocket exhaust plumes. This heating is due to radiation from the plume and to convection from the gases forced back toward the base. The latter effect begins to occur at altitudes where the ambient pressure has decreased substantially and spread of engine jet results in flow interactions. The rise in pressure due to slowing of the exhaust gases in the interaction regions causes hot gases to flow toward the vehicle. Such flow reversals occur in the center of a cluster of engines. In contrast, the base regions outside the cluster are subjected primarily to radiative heating. Optimal design of the required protection from heating in these regions might be achieved if the actual magnitude of this radiative energy transfer could be predicted. The present work describes an analytical attempt to calculate the radiative energy transfer from rocket exhaust plumes to the base regions by use of idealized physical models.

There exist no previous investigations of this problem in the literature. However, a class of similar but little related problems been considered by Schmidt,[1] and very recently by Gray and Penner.[2] They were concerned with the radiative energy transfer to centrally located base areas in cylindrical and conical gray-gas bodies.

The physical models under the present investigation are semi-infinite cylindrical and infinite conical gas bodies of uniform temperature and composition, with their axes perpendicular to the base plane. The lower portion of the gas body is shielded by a cold opaque surface, which simulates the rocket nozzle. The gas body emits and absorbs radiation, and is separated from its outer base region by a non-absorbing medium.

Scattering of radiation is assumed to be negligible. The results are presented in terms of the local apparent emissivity from the gas body to a differential area in the outer regions of the base plane. The apparent emissivity in the present case is defined as the ratio of the radiative energy flux arriving per unit area and time to that of a black surface at the same temperature. In general, it is a function of the cone angle which is zero for a cylindrical gas body, the absorption coefficient of the gas, the height of shielding, and the radial distance in the base plane from the gas body.

Presented first in the report are certain general considerations of the problem. The integral expression of the spectral apparent emissivity is modified in terms of dimensionless governing parameters. The conventional coordinate system is then transformed to a system which is convenient for direct or numerical integration. An approximate method utilizing the concept of mean path length is suggested for the calculation of the total apparent emissivity if the absorption spectrum of the gas is given. In calculating the spectral apparent emissivities, direct integration appears to be infeasible for the general case. The solution, however, for the special case of black cylindrical and conical gas bodies can be achieved. In addition, asymptotic expressions of the spectral apparent emissivity are given for a cylindrical gas body of small absorption coefficient. Results of the spectral apparent emissivity for different values of dimensionless governing parameters were computed numerically and are presented in graphical form. The spectral apparent emissivity is the same as the total apparent emissivity if a gray-gas behavior is assumed for the gas body. The gray-gas assumption has been

widely used in most gaseous-radiation studies; however, its validity is always under question and is very difficult to assess. Calculation of the total apparent emissivity by use of a mean path length is shown to be feasible for the semi-infinite cylindrical gas body with a given infrared absorption spectrum. As an illustration, numerical results of the total apparent emissivity are presented for semi-infinite cylindrical bodies of $CO_2$ (2500°F, 1 atm) and $H_2O$ (2000°F, 1 atm) by use of the existing spectral absorption data.[3,4] The implication of these calculations with respect to the gray-gas assumption is discussed.

## GENERAL CONSIDERATIONS

Consider an arbitrary gas body of uniform temperature and composition, emitting and absorbing radiative energy. The gas body is separated from a differential area $dA$ by a nonabsorbing medium. No scattering of radiation exists in the system. For a spherical coordinate system as shown in Fig. 1, the radiative energy flux incident per unit area of $dA$ and time, in the wavelength interval between $\lambda$ and $\lambda + d\lambda$ is,[5]

$$Q_\lambda = \int_\beta \int_\varphi I_{b\lambda} \left(1 - e^{-a_\lambda s}\right) \sin\beta \cos\beta \, d\beta \, d\varphi \qquad (1)$$

where $I_{b\lambda}$ is the spectral black-body intensity, $a_\lambda$ is the linear spectral absorption coefficient, and the path length $s$ is in general a function of the gas body shape, the location irradiated, the azimuth angle $\varphi$ and the polar angle $\beta$. In the present study of semi-infinite cylindrical and infinite conical gas bodies as shown in Fig. 2, $s = s(\alpha, h, r, \varphi, \beta)$, where $\alpha$ is the cone angle, $h$ is the height of

shielding, and $r$ is the radial distance in the base plane from the symmetrical axis. Defining the spectral apparent emissivity, $\epsilon_\lambda$, as the ratio of the radiative energy flux $Q_\lambda$ to that of a black body at the same temperature, there follows

$$\epsilon_\lambda = \frac{1}{\pi} \int_\beta \int_\varphi (1 - e^{-a_\lambda s}) \sin\beta \cos\beta \, d\beta \, d\varphi \tag{2}$$

For semi-infinite cylindrical and infinite conical gas bodies, $\epsilon_\lambda = \epsilon_\lambda(\alpha, h, r, a_\lambda)$.

For calculations of different physical cases, it is highly desirable to have all the governing parameters in Eq. (2) in dimensionless form. In the present case the dimensionless governing parameters are best defined as:

$$\alpha \equiv \alpha \qquad H \equiv \frac{h}{r_e} \qquad R \equiv \frac{r}{r_e} \qquad A_\lambda \equiv a_\lambda \, r_e \tag{3}$$

where $r_e$ is the bottom radius of the unshielded portion of gas body, which corresponds to the exit radius of the rocket nozzle. Accordingly,

$$S \equiv \frac{s}{r_e} = S(\alpha, H, R, \varphi, \beta) \tag{4}$$

and

$$\epsilon_\lambda = \epsilon_\lambda(\alpha, H, R, A_\lambda) \tag{5}$$

In terms of dimensionless parameters, Eq. (2) becomes

$$\epsilon_\lambda = \frac{1}{\pi} \int_\beta \int_\varphi (1 - e^{-A_\lambda S}) \sin\beta \cos\beta \, d\beta \, d\varphi \tag{6}$$

Equation (6) can be rearranged into a different form as

$$\epsilon_\lambda = F - \epsilon_{\lambda c} \tag{7}$$

where

$$F \equiv \frac{1}{\pi} \int_\beta \int_\varphi \sin\beta \cos\beta \, d\beta \, d\varphi \tag{8}$$

and

$$\epsilon_{\lambda c} \equiv \frac{1}{\pi} \int_\beta \int_\varphi e^{-A_\lambda S} \sin\beta \cos\beta \, d\beta \, d\varphi \tag{9}$$

It is readily seen from Eq. (8) that $F$ is the configuration factor, or in the present case the black-gas apparent emissivity. Consequently, $\epsilon_{\lambda c}$ can be regarded as the contribution due to the finite absorption coefficient of the gas body. It should be emphasized, however, that $\epsilon_{\lambda c}$ is still a function of configuration. Equation (7) combined with Eqs. (8) and (9) offers a slightly different physical interpretation of apparent emissivity.

Equations (8) and (9) can be written in a more convenient form for integration purposes. This is accomplished by introducing $\beta'$ in place of $\beta$. From Fig. 1, the relationship among $\varphi$, $\beta$ and $\beta'$ can be shown to be

$$\tan\beta = \sec\varphi \tan\beta' \tag{10}$$

The functions $F$ and $\epsilon_{\lambda c}$ become respectively

$$F = \frac{1}{\pi} \int_{\beta'} \int_\varphi \frac{\cos^2\varphi \tan\beta' \sec^2\beta'}{(\cos^2\varphi + \tan^2\beta')^2} \, d\beta' \, d\varphi \tag{11}$$

and

$$\epsilon_{\lambda c} = \frac{1}{\pi} \int_{\beta'} \int_\varphi e^{-A_\lambda S} \frac{\cos^2\varphi \tan\beta' \sec^2\beta'}{(\cos^2\varphi + \tan^2\beta')^2} \, d\beta' \, d\varphi \tag{12}$$

Direct integration of Eqs. (11) and (12) is in general difficult, if not impossible. Further complication arises if the shielding is considered.

The total apparent emissivity is given as

$$\epsilon = \frac{\int_0^\infty \epsilon_\lambda E_{b\lambda} \, d\lambda}{\int_0^\infty E_{b\lambda} \, d\lambda} = \frac{\pi c_1}{\sigma T^4} \int_0^\infty \frac{\epsilon_\lambda \, d\lambda}{\lambda^5 [\exp(c_2/\lambda T) - 1]} \tag{13}$$

where $E_{b\lambda}$ is the spectral black-body emissive power, $\sigma = 5.67 \times 10^{-5}$ erg/cm$^2$K$^4$sec is the Stefan-Boltzmann constant, $T$ is the temperature of the gas body, and $c_1 = 1.19 \times 10^{-5}$ cm$^2$erg/sec and $c_2 = 1.44$ cm K are the first and second radiation constants in Planck's distribution law. When one makes the gray-gas assumption as in many of the previous gaseous-radiation studies, the spectral absorption coefficient $a_\lambda$ is substituted for by an effective absorption coefficient independent of wavelength, and consequently, $\epsilon = \epsilon_\lambda$. There exists no sound basis for this assumption, and the accuracy of the final result depends entirely on the empirical choice of an effective wavelength-independent absorption coefficient. In many cases, the use of the gray-gas assumption is inevitable because of insufficient knowledge of the infrared absorption spectrum of the gaseous medium. The next question, however, is whether the total apparent emissivity can be calculated when the infrared absorption spectrum is known by either experimental or theoretical means. For the present study, an approximate method for calculating the total apparent emissivity is suggested in the following.

The integral expression of $\epsilon_\lambda$ in Eq. (6), combined with the definition of $F$ in Eq. (8), suggests the possible existence of an approximate form for $\epsilon_\lambda$:

$$\epsilon_\lambda = F\,(1 - e^{-A_\lambda L}) \tag{14}$$

where $L = L(\alpha,H,R)$ can be interpreted as the dimensionless mean path length of the gas body viewed from the base plane. The independent nature of $L$ with respect to $A_\lambda$ is actually an assumption and can only be justified by comparing the actual value of $\epsilon_\lambda$ from Eq. (6) with that from Eq. (14) by use of a properly chosen function $L(\alpha,H,R)$. It appears that the choice of $L$ is of the same nature as the choice of an effective absorption coefficient in the gray-gas assumption. However, in certain specific cases as will be shown later, a proper choice of $L$ can be achieved through analytical considerations.

Substitution of Eq. (14) into Eq. (13) gives the total apparent emissivity $\epsilon$ as:

$$\epsilon = \frac{\pi c_1 F}{\sigma T^4} \int_0^\infty \frac{[1 - \exp(-A_\lambda L)]\, d\lambda}{\lambda^5[\exp(c_2/\lambda T) - 1]} \tag{15}$$

If, at certain thermodynamic conditions, the infrared absorption spectrum is known theoretically or experimentally, the local apparent emissivity $\epsilon(\alpha,H,R)$ can be obtained by evaluating the integral in Eq. (15) numerically. The absorption spectrum can be approximated by assuming a constant value of spectral absorption coefficient over a narrow range of wavelength, and thus Eq. (15) becomes

$$\epsilon(\alpha,H,R) = \frac{\pi c_1 F}{\sigma T^4} \sum_i [1 - \exp(-A_i L)] \int_{\lambda_{1i}}^{\lambda_{2i}} \frac{d\lambda}{\lambda^5[\exp(c_2/\lambda T) - 1]} \tag{16}$$

where the summation holds all over the subdivided ranges of wavelength.

Equation (16) may be written as

$$\epsilon(\alpha,H,R) = F \sum_i [1 - \exp(-A_i L)](D_{2i} - D_{1i}) \qquad (17)$$

where the functions

$$D_{ni}(\lambda_{ni},T) \equiv \frac{1}{\sigma T^4} \int_0^{\lambda_{ni}} \frac{\pi c_1 \, d\lambda}{\lambda^5[\exp(c_2/\lambda T)-1]} \qquad (n = 1,2) \qquad (18)$$

are called the relative cumulative spectral radiance of a black body, and are tabulated as a function of temperature and frequency.[6]

For most systems of physical interest, $(\lambda T) < 0.3$ cm°K, and the Planck's distribution law can be approximated by Wien's law with an accuracy better than 1%.[7] The total apparent emissivity in this case becomes

$$\epsilon(\alpha,H,R) = \frac{\pi c_1 F}{\sigma T^4} \sum_i [1-\exp(-A_i L)] \int_{\lambda_{1i}}^{\lambda_{2i}} \lambda^{-5} e^{-c_2/\lambda T} \, d\lambda \qquad (19)$$

or by performing the integration,

$$\epsilon(\alpha,H,R) = \frac{\pi c_1 F}{\sigma} \sum_i [1-\exp(-A_i L)] \left\{ [\exp(-c_2/\lambda_{2i}T)] \times \right.$$

$$\left[ \frac{1}{c_2(\lambda_{2i}T)^3} + \frac{3}{c_2^2(\lambda_{2i}T)^2} + \frac{6}{c_2^3(\lambda_{2i}T)} + \frac{6}{c_2^4} \right] - [\exp(c_2/\lambda_{1i}T)] \times$$

$$\left. \left[ \frac{1}{c_2(\lambda_{1i}T)^3} + \frac{3}{c_2^2(\lambda_{1i}T)^2} + \frac{6}{c_2^3(\lambda_{1i}T)} + \frac{6}{c_2^4} \right] \right\} \qquad (20)$$

## SPECTRAL APPARENT EMISSIVITY OF A SEMI-INFINITE CYLINDRICAL GAS BODY ($\alpha = 0$)

For the case of a semi-infinite cylinder viewed from its outer base, the configuration factor defined in Eq. (11) can be written as:

$$F = \frac{2}{\pi} \int_0^{\beta'_o} \int_0^{\varphi_o} \frac{\cos^2\varphi \tan\beta' \sec^2\beta'}{(\cos^2\varphi + \tan^2\beta')^2} \, d\beta' \, d\varphi \tag{21}$$

where

$$\varphi_o = \sin^{-1}\left(\frac{1}{R}\right) \tag{22}$$

and

$$\beta'_o = \frac{1}{2}\left[\tan^{-1}\left(\frac{R-1}{H}\right) + \tan^{-1}\left(\frac{R^2-1}{RH}\right)\right] \tag{23}$$

Equation (21) can be integrated directly by first integrating with respect to $\tan^2\beta'$ instead of $\beta'$, and the result is

$$F(H,R) = \frac{1}{\pi} \sin\beta'_o \tan^{-1}(\sin\beta'_o \tan\varphi_o) \tag{24}$$

The same expression can also be obtained by use of the tabulated result of a more general configuration (Configuration P-2) in Ref. 8. In obtaining Eq. (24), an approximation is found necessary for the limit of $\beta'$ in the integration. The upper limit $\beta'_o$ as illustrated in Fig. 3 is being approximated as the arithmetic mean of the two limiting angles, $\beta'_1$ and $\beta'_2$, for the partially viewed region due to shielding. The error resulting from this approximation is in general quite small for a semi-infinite cylinder, and becomes smaller as $R$ increases, since the two limiting angles for the partially viewed region are getting closer.

In the limiting case $\beta'_o = \frac{\pi}{2}$ (corresponding to $H = 0$), an exact result is obtained for Eq. (24) with no shielding,

$$F(0,R) = \frac{1}{\pi} \sin^{-1}\left(\frac{1}{R}\right) \tag{25}$$

The term $\epsilon_{\lambda c}$ defined in Eq. (12) can be expressed from simple geometrical considerations as:

$$\epsilon_{\lambda c}(H,R) = \frac{2}{\pi} \int_0^{\beta_o'} \int_0^{\varphi_o} e^{-A_\lambda S} \frac{\cos^2\varphi \tan\beta' \sec^2\beta'}{(\cos^2\varphi + \tan^2\beta')^2} d\beta' d\varphi \tag{26}$$

where the dimensionless path length as shown in Fig. 3 is given by

$$S(R,\beta,\varphi) = \frac{2}{\sin\beta} (1-R^2 \sin^2\varphi)^{1/2} \tag{27}$$

or in terms of $\beta'$ and $\varphi$,

$$S(R,\beta',\varphi) = \frac{2}{\tan\beta'} (1-R^2 \sin^2\varphi)^{1/2} (\cos^2\varphi + \tan^2\beta')^{1/2} \tag{28}$$

and $\varphi_o$ and $\beta_o'$ are given in Eqs. (22) and (23), respectively. The same approximation of the limit of $\beta_o'$ as mentioned before is also introduced in Eq. (26). In general, direct integration of Eq. (26) is not feasible and numerical computation must be performed. A more convenient form for numerical computation can be achieved by introducing the variable

$$P \equiv \frac{2A_\lambda (1-R^2 \sin^2\varphi)^{1/2}}{\tan\beta'} (\cos^2\varphi + \tan^2\beta')^{1/2} \tag{29}$$

Thus, Eq. (26) reduces to

$$\epsilon_{\lambda c}(H,R) = -\frac{2}{\pi} \int_0^{\varphi_o} 4A_\lambda^2 (1-R^2 \sin^2\varphi) \int_\infty^{P_o(\varphi)} \frac{e^{-P}}{P^3} dP d\varphi \tag{30}$$

After integration by parts with respect to P, there results

$$\epsilon_{\lambda c}(H,R) = \frac{\tan^2\beta_o'}{\pi} \int_0^{\varphi_o} \frac{\Phi(P_o)\, d\varphi}{(\cos^2\varphi + \tan^2\beta_o')} \tag{31}$$

where

$$P_o(\varphi) \equiv \frac{2A_\lambda (1-R^2 \sin^2\varphi)^{1/2}}{\tan \beta_o'} \cdot (\cos^2\varphi + \tan^2\beta_o')^{1/2} \tag{32}$$

and

$$\Phi(P) = e^{-P} - P\cdot e^{-P} - P^2 \int_{-\infty}^{P} \frac{e^{-P}}{P}\, dP \tag{33}$$

The function $\Phi(P)$ has been tabulated by Schmidt.[1]

The integral appearing in Eq. (31) still must be evaluated numerically at different locations specified by H and R. Two asymptotic expressions for $\epsilon_{\lambda c}$, however, can be obtained through direct integration. In the case of no shielding (H = 0), the asymptotic expression of $\epsilon_\lambda$ for $A_\lambda \ll 1$ is given as (Appendix A):

$$\epsilon_\lambda(0,R) = \frac{4A_\lambda}{\pi} \left[ R\, E_2\left(\frac{\pi}{2}, \frac{1}{R}\right) - \left(\frac{R^2-1}{R}\right) E_1\left(\frac{\pi}{2}, \frac{1}{R}\right) \right] \tag{34}$$

where $E_1$ and $E_2$ are the elliptic integrals of the first and second kinds, respectively. For large R, the spectral apparent emissivity can be expressed as

$$\epsilon_\lambda(0,R) = \frac{A_\lambda}{R} \tag{35}$$

For the case with shielding ($H \neq 0$), the result for $A_\lambda \ll 1$ and $R \gg 1$ can be derived as (Appendix B):

$$\epsilon_\lambda(H,R) = \frac{A_\lambda}{R} \sin\beta_o' \tag{36}$$

If there is no shielding ($H = 0$, $\beta_o' = \pi/2$), it gives the expression in Eq. (35) as expected.

Numerical results for the spectral apparent emissivity in the base plane of a semi-infinite cylindrical gas body are presented in Figs. 4, 5, 6, and 7. Values of the spectral apparent emissivity, $\epsilon_\lambda$, were plotted versus R, the distance from central axis of the gas body in radii, for different values of H and $A_\lambda$. Four values of the dimensionless height of shielding, H, are given, H = 0, 1, 2, and 4, and three values are used for the dimensionless absorption coefficient, $A_\lambda$ = 0.1, 0.4, $\infty$ (black-body case). The black-body curves $(A_\lambda \to \infty)$ were calculated directly from Eq. (24), while the others were obtained through numerical integration of Eq. (26) by use of a 7090 Digital Computer.

For most practical applications, the range of R would probably be less than 5, and the spectral apparent emissivity in the base plane is about 0.1 or less, depending on the height of shielding. The effect of shielding on the spectral apparent emissivity is shown to be significant for a large spectral absorption coefficient, especially in the close vicinity of the gas body.

Asymptotic variations of the spectral emissivity for a gas body of small spectral absorption coefficient $(A_\lambda \ll 1)$ and without shielding (H = 0) were calculated from the analytical expression, Eq. (34), and are compared in Fig. 8 with the numerical results from the computer. It is clearly indicated that the analytical expression Eq. (34) can be confidently used to compute $\epsilon_\lambda$ for cases when $A_\lambda < 0.1$. In Fig. 9, a comparison is made between the asymptotic results for $A_\lambda \ll 1$ and $R \gg 1$ calculated from Eq. (36) and the computer results. Again, it is shown that Eq. (36) can be used for cases when $A_\lambda < 0.1$ without introducing appreciable errors.

It should be emphasized again that all the results and discussion in this section are directly applicable to the calculation of the total apparent emissivity if the gray-gas assumption is employed. In that case, $A_\lambda = A$, and $\epsilon_\lambda = \epsilon$.

## SPECTRAL APPARENT EMISSIVITY OF AN INFINITE CONICAL GAS BODY

For an infinite conical gas body of apex angle $2\alpha$, the configuration factor can be written as

$$F(\alpha,H,R) = \frac{2}{\pi} \int_{-\alpha}^{\beta'_o} \int_{o}^{\varphi_o} \frac{\cos^2\varphi \tan\beta' \sec^2\beta'}{(\cos^2\varphi + \tan^2\beta')^2} \, d\beta' \, d\varphi \qquad (37)$$

From Fig. 10 it can be seen that at a certain location in the base plane, the upper limit $\varphi_o(\beta')$ depends upon whether there exist tangents or asymptotes to the conical body for various values of $\beta'$. For calculating the configuration factor in both the asymptote and tangent regions, Eq. (37) can be split into two main integrations as

$$\begin{aligned} F(\alpha,H,R) &= \frac{2}{\pi} \int_{\beta'_c}^{\beta'_o} \int_{o}^{\varphi_{ot}} \frac{\cos^2\varphi \tan\beta' \sec^2\beta'}{(\cos^2\varphi + \tan^2\beta')^2} \, d\beta' \, d\varphi \\ &\quad + \frac{2}{\pi} \int_{-\alpha}^{\beta'_c} \int_{o}^{\varphi_{oa}} \frac{\cos^2\varphi \tan\beta' \sec^2\beta'}{(\cos^2\varphi + \tan^2\beta')^2} \, d\beta' \, d\varphi \\ &\equiv F_1 + F_2 \end{aligned} \qquad (38)$$

where $F_1$ and $F_2$ represent the first and second integrals, respectively, $\beta'_c$ is the critical angle at which the tangent gives way to the asymptote, and $\varphi_{ot}$ and $\varphi_{oa}$ are the limiting azimuth angles in the tangent and

asymptote regions, respectively. The expression for $\varphi_{ot}$, which defines the limit of integration, can be obtained by setting the expression of the path length (Appendix C) equal to zero, and the result is

$$\varphi_{ot}(\beta') = \tan^{-1}\left\{\frac{R \tan\alpha \cot\beta' + (1-H\tan\alpha)}{[R^2-(1-H\tan\alpha)^2]^{1/2}}\right\} \tag{39}$$

In the asymptote region, the conic section is always a hyperbola, and the asymptote to the hyperbola determines the limit of $\varphi_{oa}$,

$$\varphi_{oa}(\beta') = \cos^{-1}\left(\frac{\tan\beta'}{\tan\alpha}\right) \tag{40}$$

The critical angle $\beta'_c$ is determined by realizing that Eqs. (39) and (40) must be identical at $\beta'_c$, and the result is

$$\beta'_c = -\tan^{-1}\left[\frac{(1-H\tan\alpha)\tan\alpha}{R}\right] \tag{41}$$

Again, the upper limiting angle $\beta'_o$ in Eq. (38) has been approximated by the arithmetic mean of the two limiting angles $\beta'_1$ and $\beta'_2$, and it is (see Appendix D),

$$\beta'_o = \frac{1}{2}\left\{\tan^{-1}\left(\frac{R-1}{H}\right) + \tan^{-1}\left[\frac{R\sqrt{R^2-1}\tan\alpha}{\sqrt{R^2-(1-H\tan\alpha)^2}-(1-H\tan\alpha)\sqrt{R^2-1}}\right]\right\} \tag{42}$$

As shown in Fig. 10, the tangents to the cone for various values of $\beta'$ ($\beta'_c \le \beta' \le \beta'_o$) trace a plane. The inclination angle $\theta$ of the plane to the cone axis, is a function of the space variables of the location irradiated. The angle $\theta$ is found to be equal to $\beta'_c$,

$$\theta = -\tan^{-1}\left[\frac{(1-H\tan\alpha)\tan\alpha}{R}\right] = \beta_c' \tag{43}$$

The configuration factor of the triangular plane mentioned above has also been given in Ref. 8 [Eq. (6), Fig. 2] as of the following form

$$F_1 = \frac{2\cos^2\theta}{\pi}\int_y\int_x \frac{r_o\, y\, dx\, dy}{(x^2 + y^2 + r_o^2 + 2r_o y \sin\theta)^2} \tag{44}$$

where $x$ measures the distance from the plane axis, $y$ is the distance along the plane axis from the vertex, and $r_o$ is the distance from the plane to the viewed area in the base plane. In dimensionless form, Eq. (44) becomes

$$F_1 = \frac{2R_o\cos^2\theta}{\pi}\int_Y\int_X \frac{Y\, dY\, dX}{(X^2 + Y^2 + R_o^2 + 2R_o Y \sin\theta)^2} \tag{45}$$

where

$$X \equiv \frac{x}{r_e} \quad , \quad Y \equiv \frac{y}{r_e} \quad , \quad R_o \equiv \frac{r_o}{r_e} \tag{46}$$

as indicated in Fig. 10. The dimensionless distance $R_o$, in the present case, may be expressed by:

$$R_o = \frac{R^2-(1-H\tan\alpha)^2}{R} \tag{47}$$

The two expressions for $F_1$, the configuration factor in the asymptote region, in Eqs. (38) and (45) are actually identical. The geometrical relations between two sets of integration variables, $\beta'$, $\varphi$, and $X$, $Y$, can be derived from Fig. 10 as

$$\tan \beta' = \frac{\tan \alpha \{R-[(1-H \tan \alpha)(\tan \alpha)Y/C]\}}{[R\, Y(\tan \alpha)/C - (1-H \tan \alpha)]} \tag{48}$$

and

$$\tan \varphi = \frac{X}{R - [(1-H \tan \alpha)(\tan \alpha)Y/C]} \tag{49}$$

where

$$C \equiv \sqrt{R^2 + (1-H \tan \alpha)^2 \tan^2 \alpha} \tag{50}$$

By use of the above relations, Eq. (38) becomes

$$F(\alpha,H,R) = F_1 + F_2 = \frac{2R_o \cos^2 \theta}{\pi} \left\{ \int_{Y_o}^{\infty} \int_{X=0}^{BY(\tan \alpha)/C} \frac{Y\, dX\, dY}{(X^2+Y^2+R_o^2+2R_o Y \sin \theta)^2} \right.$$

$$\left. + \int_{\infty}^{-C/\tan\alpha} \int_{o}^{B\sqrt{Y^2\tan^2\alpha - C^2}/C} \frac{Y\, dX\, dY}{(X^2+Y^2+R_o^2+2R_o\, Y \sin \theta)^2} \right\} \tag{51}$$

where $Y_o$ is the dimensionless distance, measured from the vertex to the point corresponding to $\beta_o'$ :

$$Y_o \equiv \frac{1}{\cos \theta} [\bar{H} + (\cot \alpha - H)] \tag{52}$$

$$B \equiv \sqrt{R^2-(1-H \tan \alpha)^2} \tag{53}$$

and $\bar{H}$ is the axial distance, measured from the base plane, due to shielding, and is given by

$$\bar{H} \equiv \frac{R^2 - (1-H \tan \alpha)^2}{R \tan \beta_o' + (1-H \tan \alpha) \tan \alpha} \tag{54}$$

Direct integration of the first integral in Eq. (51) is given in Appendix E, and the result is

$$F_1 = \frac{1}{\pi C}\left[(1-H\tan\alpha)\tan\alpha\right]\tan^{-1}\left(\frac{B\tan\alpha}{C}\right) - \frac{1}{\pi M}\left[R^2 - \bar{H}(1-H\tan\alpha)\tan\alpha - 2(1-H\tan\alpha)^2\right] \times \tan^{-1}\left\{\frac{B}{M}\left[(1-H\tan\alpha) + \bar{H}\tan\alpha\right]\right\} +$$

$$\frac{B\tan\alpha}{2\sqrt{R^2+B^2\tan^2\alpha}} - \frac{B\tan\alpha}{\pi\sqrt{R^2+B^2\tan^2\alpha}}\tan^{-1}\left\{\frac{(R^2/B^2)\bar{H}\sec^2\alpha - (1-H\tan\alpha)\left[1-\left(\frac{R^2}{B^2}\right)\csc^2\alpha\right]\tan\alpha}{\sqrt{R^2+B^2\tan^2\alpha}}\right\} \tag{55}$$

where

$$M \equiv \sqrt{\left[\bar{H} + \frac{1-H\tan\alpha}{\tan\alpha}\right]^2 R^2 + \left[(1-H\tan\alpha)\bar{H}\tan\alpha - R^2 + 2(1-H\tan\alpha)^2\right]^2} \tag{56}$$

Similarly, the configuration factor $F_2$ for the asymptote region, given by the second integral in Eq. (51), can be integrated once, giving

$$F_2 = \frac{(1-H\tan\alpha)\tan\alpha}{\pi C}\tan^{-1}\left(\frac{B}{C}\tan\alpha\right) + \frac{B}{\pi C}\int_{-C/\tan\alpha}^{\infty} \frac{(YR_o\tan^2\alpha + C^2\sin\theta)\,dY}{\sqrt{Y^2\tan^2\alpha - C^2}\left[\frac{R^2Y^2\sec^2\alpha}{C^2} + 2R_oY\sin\theta + R_o^2 - B^2\right]} \tag{57}$$

The second term in the right hand side of the above equation can be integrated directly only for two special cases. In the first case, when the base plane is located at the vertex of the cone, $1-H\tan\alpha = 0$, $\theta = 0$ and $F_2$ is given by

$$F_2 = \frac{\sin^2\alpha}{2} \tag{58}$$

In the second case, an asymptotic result for $R \gg 1$ can be derived. This is

$$F_2 = \frac{B^3}{R} \frac{\sin^2\alpha}{2} \frac{1}{[R^4 - B^2(1-H\tan\alpha)^2\tan^2\alpha]^{1/2}} \tag{59}$$

Note that, as $R \to 1$ and $H \to 0$, $F_2 \to 0$.

In calculating the term $\epsilon_{\lambda c}$, consideration should also be given to the two separate regions, the tangent and asymptote regions. Thus

$$\epsilon_{\lambda c}(H,R,\alpha) = \frac{2}{\pi} \int_{\beta_c'}^{\beta_o'} \int_{o}^{\varphi_{ot}} e^{-A_\lambda S} \frac{\cos^2\varphi \tan\beta' \sec^2\beta'}{(\cos^2\varphi + \tan^2\beta')^2} \, d\beta' \, d\varphi$$

$$+ \frac{2}{\pi} \int_{-\alpha}^{\beta_c'} \int_{o}^{\varphi_{oa}} e^{-A_\lambda S} \frac{\cos^2\varphi \tan\beta' \sec^2\beta'}{(\cos^2\varphi + \tan^2\beta')^2} \, d\beta' \, d\varphi$$

$$\equiv \epsilon_{\lambda c_1} + \epsilon_{\lambda c_2} \tag{60}$$

where $\epsilon_{\lambda c_1}$ and $\epsilon_{\lambda c_2}$ represent the first and second integrals, respectively. The dimensionless path length can be derived from geometrical analysis (Appendix C) as

$$S = \frac{2(\cos^2\varphi + \tan^2\beta')^{1/2}\cos\varphi}{(\tan^2\beta' - \tan^2\alpha\cos^2\varphi)} \times$$

$$\left\{\frac{\tan^2\beta'}{\cos^2\varphi}[(1-H\tan\alpha)^2 - R^2\sin^2\varphi] + 2R(1-H\tan\alpha)\tan\beta'\tan\alpha + R^2\tan^2\alpha\right\}^{1/2} \tag{61}$$

The above expression holds in the tangent region $(\beta_c' \leq \beta' \leq \beta_o')$, excluding the region where $\beta < \alpha$, in which the path length S goes to infinity. In the asymptote region $(-\alpha \leq \beta' \leq \beta_c')$, S is infinite for all $\varphi$, therefore $\epsilon_{\lambda c_2} = 0$. As a direct consequence, in the region $R \leq |(1-H \tan \alpha)|$ in the base plane, the asymptote region extends all over the cone and $\epsilon_{\lambda c}$ approaches to zero regradless of the value of the absorption coefficient.

In general, the term $\epsilon_{\lambda c}$ has the expression

$$\epsilon_{\lambda c}(H,R,\alpha) = \frac{2}{\pi} \int_{\beta_c'}^{\beta_o'} \int_{o}^{\varphi_{ot}} e^{-A_\lambda S} \frac{\cos^2\varphi \tan\beta' \sec^2\beta'}{(\cos^2\varphi + \tan^2\beta')^2} d\beta' d\varphi \tag{62}$$

where $\varphi_{ot}$, $\beta_o'$ and S are given in Eqs. (39), (42), and (61), respectively.

Numerical results of the spectral apparent emissivity are shown in Figs. 11 through 22, for $\alpha = 10°, 30°, 60°$, $A_\lambda = 0.1, 0.4, \infty$, and $H = 0, 1, 2, 4$. The values of the configuration factor F (or $\epsilon_\lambda$ when $A_\lambda \to \infty$) were obtained by adding $F_1$ calculated from the analytical expressions in Eq. (55) and $F_2$ calculated numerically from Eq. (57). For finite values of $A_\lambda$, the spectral apparent emissivity is the difference between F and $\epsilon_{\lambda c}$, the latter being numerically computed from Eq. (62). All numerical computations were performed by the use of a 7090 Digital Computer.

As would be expected, at a certain location in the base plane, the spectral apparent emissivity is larger for the conical gas body $(\alpha > 0)$ than that for the cylindrical gas body $(\alpha = 0)$ of the same absorption

coefficient $A_\lambda$, and is increasing with the cone angle. Furthermore, as the cone angle increases, the effect of finite absorption coefficients is diminishing and the spectral apparent emissivity approaches to its black-body value or the configuration factor. This is due to the fact that the asymptote region, which is eventually black in the sense of infinite path length, becomes larger and larger as compared to the tangent region, in which the effect of finite absorption exists. In the limiting case when $R \leq |(1-H \tan \alpha)|$ as mentioned before, the asymptote region extends all over the cone, and $\epsilon_\lambda = F$ for all values of $A_\lambda$. This is clearly shown in Figs. 20, 21, and 22.

## CALCULATION OF TOTAL APPARENT EMISSIVITY OF A SEMI-INFINITE CYLINDRICAL GAS BODY

The present section will try to demonstrate the method of calculating the total apparent emissivity by utilizing the concept of mean path length. This concept has been widely used in various calculations of gaseous radiative energy transfer. But the present case is different from all other previous calculations in that the present mean path length is a complicated function of the space variables, which characterize the location in the base plane. The following calculation of the total apparent emissivity in the base plane is based on a semi-infinite cylindrical gas body. In this case, an approximate expression of the mean path length can be established semi-empirically through analytical considerations. For an infinite conical gas body, such an expression would be entirely empirical.

Consider first a semi-infinite cylindrical gas body of a sufficiently small absorption coefficient so that $A_\lambda L \ll 1$. Therefore,

Therefore, Eq. (14) may be approximated as

$$\epsilon_\lambda = F(1 - e^{-A_\lambda L}) \approx FA_\lambda L \tag{63}$$

Comparing the above equation with the asymptotic expression of $\epsilon_\lambda$ for $H = 0$ and $A_\lambda \ll 1$, Eq. (34), and using the exact result of $F$ in Eq. (25), one can find

$$L(0,R) = \frac{4}{\sin^{-1}\left(\frac{1}{R}\right)} \left[ R\, E_2\left(\frac{\pi}{2}, \frac{1}{R}\right) - \left(\frac{R^2-1}{R}\right) E_1\left(\frac{\pi}{2}, \frac{1}{R}\right) \right] \tag{64}$$

It should be emphasized that the above expression is valid for all values of $R$, but under the limitations, $H = 0$ and $A_\lambda \ll 1$. The condition $A_\lambda L \ll 1$ is eliminated above, since $L$ as calculated from Eq. (64) (see Fig. 23) is of the order $O[1]$. Furthermore, a numerical check reveals that the values of $\epsilon_\lambda$ obtained by use of the mean path length, Eq. (14) and Eq. (64), agree very well with the numerically calculated results for all values of $A_\lambda$. It is also obvious that the agreement becomes exact at two limits, $A_\lambda = 0$ and $A_\lambda \to \infty$. This indicates that the restriction of $A_\lambda \ll 1$ can also be removed, although no rigorous proof has been established here.

For the case with shielding $(H \neq 0)$ the asymptotic expression is given in Eq. (36) for $A_\lambda \ll 1$, but only for the range $R \gg 1$. Combining Eqs. (24), (36) and (63) gives

$$L = \frac{\pi}{R \tan^{-1}(\sin \beta_o' \tan \varphi_o)} \tag{65}$$

under the conditions $A_\lambda \ll 1$ and $R \gg 1$. In order to obtain an expression for all the values of $R$, a semi-empirical equation is suggested as

$$L(H,R) = \frac{4 \sin \beta_o'}{\tan^{-1}(\sin \beta_o' \tan \varphi_o)} \left[ R\, E_2\left(\frac{\pi}{2}, \frac{1}{R}\right) - \left(\frac{R^2-1}{R}\right) \right.$$

$$\left. E_1\left(\frac{\pi}{2}, \frac{1}{R}\right) + \frac{\pi}{16R^3} \cos^2 \beta_o' \right] \qquad (66)$$

The above equation is chosen based on the consideration that it should reduce to Eq. (64) as $H \to 0$, and to Eq. (65) for $A_\lambda \ll 1$, $R \gg 1$. Again, the comparison between the values of $\epsilon_\lambda$ obtained from Eqs. (14) and (66), and the numerical results from the computer indicates that the condition $A_\lambda \ll 1$ is not necessary in the present case. The values of $L$ as a function of $H$ and $R$ are plotted in Fig. 23.

With the expression of $L$ as given in Eq. (66), one can calculate the total apparent emissivity according to Eq. (17) with a given infrared absorption spectrum. By using the available absorption measurements for $CO_2$ and $H_2O$ at high temperatures as shown in Figs. 24 and 26,[3,4] numerical calculations have been performed and the results are presented in Figs. 25 and 27. At the same location in the base plane, the apparent emissivity of $H_2O$ is found to be considerably larger than that of $CO_2$. This is due to the fact that there exist more and wider $H_2O$ absorption bands in the significant wavelength region around the maximum point of the Planck's distribution. The variations of the total apparent emissivity $\epsilon$ with respect to $H$ and $R$ are similar to those of the spectral apparent emissivity $\epsilon_\lambda$. This implies that the gray-gas assumption does not change the basic character of the functional dependence on $H$ and $R$, and the assumption can be successfully employed if the wavelength-independent absorption coefficient is properly chosen. For $CO_2$ at 2500°F

and 1 atm., it is found by comparing Fig. 25 with corresponding $\epsilon_\lambda$-figures, Figs. 4 to 7, that the effective wavelength-independent coefficient A is about 0.05 for all four values of H. For $H_2O$ at 2000°R and 1 atm., the value of A is about 0.25 for different values of H.

## REFERENCES


1. E. Schmidt, Z. ver Dtsch. Ing. 77, 1162 (1933). See also M. Jakob, Heat Transfer, Vol. II, pp. 106-110, John Wiley and Sons, Inc., New York (1958).

2. L. D. Gray and S. S. Penner, "Radiative Energy Transfer to Centrally Located Areas in Cylindrical and Conical Chambers Containing Isothermal, Gray Emitters," J. Quant. Spect. Rad. Transf., 3, 29 (1963).

3. D. K. Edwards, "Absorption by Infrared Bands of Carbon Dioxide Gas at Elevated Pressures and Temperatures," J. Opt. Soc. A., 50, 130 (1960).

4. K. E. Nelson, "Experimental Determination of the Band Absorptivities of Water Vapor at Elevated Pressures and Temperatures," M. S. Thesis, Univ. of Calif., Berkeley, Calif. (1959).

5. E. R. G. Eckert and R. M. Drake, Jr., Heat and Mass Transfer, p. 388, McGraw-Hill Book Co., Inc., New York (1959).

6. N. Pivonsky, Tables of Blackbody Radiation Functions, The MacMillan Co., New York (1961).

7. S. S. Penner, Quantitative Molecular Spectroscopy and Gas Emissivities, p. 9, Chap. 19, Addison-Wesley Publishing Co., Inc., New York (1959).

8. D. C. Hamilton and W. R. Morgan, "Radiant-Interchange Configuration Factors," NACA TN-2836 (1952).

9. H. B. Dwight, Tables of Integrals and Other Mathematical Data, 4th Ed., The MacMillan Co., New York (1961).

## APPENDIX A

### Asymptotic Expression for the Spectral Apparent Emissivity of a Semi-Infinite Cylindrical Gas Body ($H = 0$, $A_\lambda \ll 1$)

The correction term $\epsilon_{\lambda c}$ for the spectral apparent emissivity of a cylindrical gas body due to finite absorption coefficient is given as

$$\epsilon_{\lambda c}(H,R) = \frac{2}{\pi} \int_0^{\beta_o'} \int_0^{\varphi_o} e^{-A_\lambda S} \frac{\cos^2\varphi \tan\beta' \sec^2\beta'}{(\cos^2\varphi + \tan^2\beta')^2} d\beta' d\varphi \tag{26}$$

where the dinensionless path length $S$ can be expressed as

$$S = \frac{2}{\tan\beta'} (1-R^2 \sin^2\varphi)^{1/2} (\cos^2\varphi + \tan^2\beta')^{1/2} \tag{28}$$

By letting

$$\eta = (\cos^2\varphi + \tan^2\beta')^{1/2} / \tan\beta' \tag{A-1}$$

Equation (26) becomes

$$\epsilon_{\lambda c}(H,R) = \frac{2}{\pi} \int_0^{\varphi_o} \int_\infty^{\eta_o} e^{-m\eta} (-\eta^{-3}) d\eta d\varphi \tag{A-2}$$

where

$$\eta_o = (\cos^2\varphi + \tan^2\beta_o')^{1/2} / \tan\beta_o' \tag{A-3}$$

and

$$m = 2 A_\lambda (1-R^2 \sin^2\varphi)^{1/2} \tag{A-4}$$

Equation (A-2) can be further written as

$$\epsilon_{\lambda c}(H,R) = \frac{2}{\pi} \int_0^{\varphi_o} d\varphi \left[ \frac{1}{2} \eta^{-2} e^{-m\eta} - \frac{m}{2} \left( \eta^{-1} e^{-m\eta} + m \int \eta^{-1} e^{-m\eta} d\eta \right) \right]_\infty^{\eta_o}$$

$$= \frac{2}{\pi} \int_0^{\varphi_o} d\varphi \left\{ \left[ \frac{1}{2} \eta^{-2} e^{-m\eta} - \frac{m}{2} \eta^{-1} e^{-m\eta} \right]_\infty^{\eta_o} - \frac{m^2}{2} \int_\infty^{\eta_o} \eta^{-1} e^{-m\eta} d\eta \right\} \tag{A-5}$$

Now consider the integral

$$\int_{\infty}^{\eta_o} \eta^{-1} e^{-m\eta} \, d\eta$$

Since $\eta_o > 1$ for the range $0 < \beta_o' < \frac{\pi}{2}$ and the integrand is always psoitive, it follows

$$\int_{\infty}^{1} \eta^{-1} e^{-m\eta} \, d\eta > \int_{\infty}^{\eta_o > 1} \eta^{-1} e^{-m\eta} \, d\eta \qquad \text{(A-6)}$$

From tables of definite integrals[9]

$$\int_{\infty}^{1} \eta^{-1} e^{-m\eta} \, d\eta = 0.577 + \ell n \, m - m + \frac{m^2}{2 \cdot 2!} \cdots \qquad \text{(A-7)}$$

When $A_\lambda \ll 1$ and consequently $m < 1$, it is obvious that Eq. (A-5) can be approximated by

$$\epsilon_{\lambda c}(H,R) = \frac{2}{\pi} \int_{o}^{\varphi_o} d\varphi \left[ \frac{1}{2} \eta^{-2} e^{-m\eta} (1-m\eta) \right]_{\infty}^{\eta_o} \qquad \text{(A-8)}$$

or

$$\epsilon_{\lambda c}(H,R) = \frac{1}{\pi} \int_{o}^{\varphi_o} \eta_o^{-2} e^{-m\eta_o} (1-m\eta_o) \, d\varphi \qquad \text{(A-9)}$$

For the case of no shielding $(H = 0, \beta_o' = \frac{\pi}{2})$, $\eta_o = 1$, and Eq. (A-9) becomes

$$\epsilon_{\lambda c}(O,R) = \frac{1}{\pi} \int_{o}^{\varphi_o} e^{-m} (1-m) \, d\varphi \qquad \text{(A-10)}$$

or, since $m \ll 1$,

$$\epsilon_{\lambda c}(O,R) = \frac{1}{\pi} \int_{o}^{\varphi_o} (1-2m) \, d\varphi \qquad \text{(A-11)}$$

From Eq. (25) and (Eq. (A-4), Eq. (A-11) gives

$$\epsilon_{\lambda c}(0,R) = F - \frac{4A_\lambda}{\pi} \int_0^{\varphi_o} (1-R^2 \sin^2\varphi)^{1/2} \, d\varphi$$

Or,

$$\epsilon_\lambda(0,R) = \frac{4A_\lambda}{\pi} \int_0^{\varphi_o} (1-R^2 \sin^2\varphi)^{1/2} \, d\varphi \qquad \text{(A-12)}$$

By letting $\sin\varphi = N$, Eq. (A-12) can be rearranged as

$$\epsilon_\lambda(0,R) = \frac{4A_\lambda}{\pi} \int_0^{1} \frac{\sqrt{(1-N^2)}}{\sqrt{(R^2-N^2)}} \, dN \qquad \text{(A-13)}$$

From integration tables,[9] it follows

$$\epsilon_\lambda(0,R) = \frac{4A_\lambda}{\pi} \left[ R\, E_2\left(\frac{\pi}{2}, \frac{1}{R}\right) - \left(\frac{R^2-1}{R}\right) E_1\left(\frac{\pi}{2}, \frac{1}{R}\right) \right] \qquad (34)$$

where $E_1(\varphi,K)$ and $E_2(\varphi,K)$ are the elliptic integrals of the first and the second kind, respectively,

$$E_1(\tau,K) = \int_0^{\tau} (1-K^2 \sin^2\psi)^{-1/2} \, d\psi \qquad \text{(A-14)}$$

and

$$E_2(\tau,K) = \int_0^{\tau} (1-K^2 \sin^2\psi)^{1/2} \, d\psi \qquad \text{(A-15)}$$

Both functions are numerically tabulated[9] for the present case $\tau = \frac{\pi}{2}$.

When $R$ is very large $(R \gg 1)$ the elliptic integrals can be approximated as[9]

$$E_1\left(\frac{\pi}{2}, \frac{1}{R}\right) = \frac{\pi}{2}\left[1 + \frac{1}{4R^2}\right] \qquad \text{(A-16)}$$

$$E_2\left(\frac{\pi}{2}, \frac{1}{R}\right) = \frac{\pi}{2}\left[1 - \frac{1}{4R^2}\right]$$

and the spectral apparent emissivity becomes

$$\epsilon_\lambda(0,R) = \frac{A_\lambda}{R} \tag{35}$$

## APPENDIX B

### Asymptotic Expression for the Spectral Apparent Emissivity of a Semi-Infinite Cylindrical Gas Body ($A_\lambda \ll 1$, $R \gg 1$)

For $A_\lambda \ll 1$, it is shown in Appendix A that

$$\epsilon_{\lambda c}(H,R) = \frac{1}{\pi} \int_0^{\varphi_o} \eta_o^{-2} e^{-m\eta_o} (1-m\eta_o)\, d\varphi \tag{A-9}$$

where the limit $\eta_o$ is given by Eq. (A-3). When $R$ is very large ($R \gg 1$), the angle $\varphi$ becomes very small and Eq. (A-3) can be approximated by

$$\eta_o = (1 + \tan^2\beta_o')^{1/2} / \tan\beta_o' = \frac{1}{\sin\beta_o'} \tag{B-1}$$

Since $\eta_o$ becomes independent of $\varphi$, Eq. (A-9) can be expressed in the following approximate form

$$\epsilon_{\lambda c}(H,R) = \frac{1}{\pi\,\eta_o^2} \int_0^{\varphi_o} (1-2m\eta_o)\, d\varphi \tag{B-2}$$

With $m$ given by Eq. (A-4), direct integration of (B-2) gives

$$\epsilon_{\lambda c}(H,R) = \frac{1}{\pi\,\eta_o^2}\,\varphi_o - \frac{A_\lambda}{\eta_o R}$$

or

$$\epsilon_{\lambda c}(H,R) = \frac{\sin^2\beta_o'}{\pi} \sin^{-1}\left(\frac{1}{R}\right) - \frac{A_\lambda}{R}\sin\beta_o' \tag{B-3}$$

From Eq. (24) the spectral apparent emissivity $\epsilon$ can be written as

$$\epsilon_\lambda(H,R) = \frac{A_\lambda}{R}\sin\beta_o' \tag{36}$$

In the case of no nozzle shielding $\left(H = 0, \quad \beta_o' = \frac{\pi}{2}\right)$, Eq. (36) becomes

$$\epsilon_\lambda(0,R) = \frac{A_\lambda}{R} \tag{35}$$

which is the same result as derived in Appendix A.

## APPENDIX C

### Derivation of the Expression for the Path Length Through a Conical Gas Body

There are two possible ways to obtain the expression for the path length through a cone. In the first case, consideration is given to the geometric properties of conic sections for different values of the angle $\beta'$, and geometric relations in plane geometry will be employed. This would eventually lead to many geometric relations in different regions of the cone according to $\beta$! The same results can be obtained in a much more direct fashion by a three-dimensional geometric analysis, as shown below.

The following derivation of the expression of path length $s$ is concerned with the region where $\beta > \alpha$, since $s \to \infty$ as $\beta < \alpha$. From Fig. (C-1), simple relations can be established as follows:

$$\tan \beta' = \frac{j}{L_1} = \frac{r + c}{L_1 + L_2} \tag{C-1}$$

$$\tan \beta = \frac{i}{L_1} = \frac{i + s'}{L_1 + L_2} \tag{C-2}$$

$$\tan \alpha = \frac{e}{L_1+(r_e \cot\alpha - h)} = \frac{d}{L_1+L_2+(r_e \cot\alpha - h)} \tag{C-3}$$

$$(i + s')^2 = b^2 + (r + c)^2 \tag{C-4}$$

and

$$e^2 = i^2 + r^2 - 2rj \tag{C-5}$$

Appropriate manipulation of Eqs. (C-1), (C-2) and (C-4) gives

$$b^2 = (L_1 + L_2)^2(\tan^2\beta - \tan^2\beta') \tag{C-6}$$

Since $d^2 = b^2 + c^2$, there results from Eqs. (C-3) and (C-6):

$$L_1+L_2 = \left\{[(r_e\cot\alpha-h)\tan^2\alpha + r\tan\beta'] + \{[(r_e\cot\alpha-h)\tan^2\alpha + r\tan\beta']^2 + \right.$$
$$\left. +[(r_e\cot\alpha-h)^2\tan^2\alpha - r^2](\tan^2\beta-\tan^2\alpha)\}^{1/2}\right\}/(\tan^2\beta-\tan^2\alpha) \quad \text{(C-7)}$$

The expression for $L_1$ can be obtained by use of Eq. (C-5), in which j, i and e are eliminated through the respective relations given in Eqs. (C-1), (C-2) and (C-3). The result is

$$L_1 = \left\{[(r_e\cot\alpha-h)\tan^2\alpha + r\tan\beta'] - \{[(r_e\cot\alpha-h)\tan^2\alpha + r\tan\beta']^2 + \right.$$
$$\left. [(r_e\cot\alpha-h)^2\tan^2\alpha - r^2](\tan^2\beta - \tan^2\alpha)\}^{1/2}\right\}/(\tan^2\beta - \tan^2\alpha) \quad \text{(C-8)}$$

Combining Eqs. (C-7) and (C-8) yields the expression for $L_2$:

$$L_2 = \frac{2\{[(r_e\cot\alpha-h)\tan^2\alpha + r\tan\beta']^2+[(r_e\cor\alpha-h)^2\tan^2\alpha - r^2](\tan^2\beta-\tan^2\alpha)\}^{1/2}}{(\tan^2\beta - \tan^2\alpha)} \quad \text{(C-9)}$$

According to Fig. (C-1), the path length s is given by

$$s = \frac{s'}{\sin\beta} = \frac{L_2\tan\beta}{\sin\beta} = \frac{L_2}{\cos\beta} \quad \text{(C-10)}$$

where $L_2$ has the expression in Eq. (C-9). In order to have s in terms of two independent parameters, $\beta'$ and $\varphi$, only, Eq. (10) must be used and the expression for s becomes

$$s = \frac{2\cos\varphi(\cos^2\varphi + \tan^2\beta')}{(\tan^2\beta' - \tan^2\alpha\cos^2\varphi)}^{1/2} \times \left\{ \frac{\tan^2\beta'}{\cos^2\varphi} [(r_e\cot\alpha - h)^2\tan^2\alpha - r^2\sin^2\varphi] + \right.$$

$$\left. + 2\, r \tan\beta'(r_e\cot\alpha - h)\tan^2\alpha + r^2\tan^2\alpha \right\}^{1/2} \qquad \text{(C-11)}$$

Therefore, the expression for the path length through a conical gas body in dimensionless form is given by

$$S = \frac{2\cos\varphi(\cos^2\varphi + \tan^2\beta')}{(\tan^2\beta' - \tan^2\alpha\cos^2\varphi)}^{1/2} \times \left\{ \frac{\tan^2\beta'}{\cos^2\varphi} [(1 - H\tan\alpha)^2 - R^2\sin^2\varphi] + \right.$$

$$\left. 2\, R \tan\beta' \tan\alpha(1 - H\tan\alpha) + R^2\tan^2\alpha \right\}^{1/2} \qquad \text{(61)}$$

## APPENDIX D

### Shielding Effect on the Integration Limit of the Spectral Apparent Emissivity of a Conical Gas Body

It can easily be shown from Fig. 10 that the lower limiting angle $\beta_2'$ corresponding to a shielding height H is given by

$$\beta_2' = \tan^{-1}\left(\frac{R-1}{H}\right) \tag{D-1}$$

Geometrically the upper limiting angle, $\beta_1'$, is the one which corresponds to the limiting angle $\varphi_{ot}$ for both of the tangents to the bottom circle of the unshielded portion and to the conic section, determined by the plane which has an inclination $\beta_1'$ to the vertical axis, and drawn from the location irradiated. The equation of the tangent to the bottom circle of the unshielded portion is simply given by

$$\tan \varphi_{ot} = \frac{1}{\sqrt{R^2 - 1}} \tag{D-2}$$

and the equation of the tangent to the conic section is given in Eq. (39), which is derived by setting the path-length expression given in Appendix C equal to zero,

$$\tan \varphi_{ot} = \frac{R \tan \alpha \cot \beta' + (1-H \tan \alpha)}{[R^2 - (1-H \tan \alpha)^2]^{1/2}} \tag{D-3}$$

Equating Eqs. (D-2) and (D-3), and solving for $\beta_1'$ gives

$$\beta_1' = \tan^{-1}\left[\frac{R\sqrt{R^2 - 1}\ \tan \alpha}{\sqrt{R^2 - (1-H \tan \alpha)^2} - (1-H \tan \alpha)\sqrt{R^2-1}}\right] \tag{D-4}$$

It is obvious that for $\beta_2' < \beta' < \beta_1'$ the range of integration on $\varphi$ is not from $0 \rightarrow \varphi_{ot}(\beta')$. A complicated expression for this range as a function of $\beta'(\beta_2' < \beta' < \beta_1')$ can be obtained, but it is so complicated that an averaging procedure is desirable. It is accomplished by considering that the range of integration is from $0 \rightarrow \varphi_o(\beta_o')$, where $\beta_o'$ is the arithmetic mean of the two limiting angles,

$$\beta_o' = \frac{1}{2}(\beta_1' + \beta_2') = \frac{1}{2}\left\{ \tan^{-1}\left(\frac{R-1}{H}\right) + \right.$$

$$\left. + \tan^{-1}\left[ \frac{R\sqrt{R^2 - 1}\ \tan\alpha}{\sqrt{R^2 - (1-H\tan\alpha)^2} - (1-H\tan\alpha)\sqrt{R^2-1}} \right] \right\} \quad (42)$$

This approximation is reasonable, since the difference between $\beta_1'$ and $\beta_2'$ is very small, especially as $R$ becomes larger.

## APPENDIX E

### Configuration Factor for the Tangent Region of a Conical Gas Body

The configuration factor for the tangent region of a conic gas body is given in Eq. (51) as

$$F_1 = \frac{2\,R_o\cos^2\theta}{\pi} \int_{Y_o}^{\infty} \int_{X=0}^{B(\tan\alpha)Y/c} \frac{Y\,dX\,dY}{(X^2+Y^2+R_o^2+2R_oY\sin\theta)^2} \qquad \text{(E-1)}$$

Integration with respect to $X^9$ yields the following expression:

$$F_1 = F_{11} + F_{12} \qquad \text{(E-2)}$$

where

$$F_{11} \equiv \frac{R_o\cos^2\theta}{\pi} \int_{Y_o}^{\infty} \frac{(B/c)Y^2\tan\alpha\,dY}{(Y^2+R_o^2+2R_oY\sin\theta)[(R^2Y^2\sec^2\alpha/C^2)+R_o^2+2R_oY\sin\theta]} \qquad \text{(E-3)}$$

and

$$F_{12} \equiv \frac{R_o\cos^2\theta}{\pi} \int_{Y_o}^{\infty} \frac{Y}{(Y^2+R_o^2+2R_oY\sin\theta)^{3/2}} \tan^{-1}\left[\frac{(B/C)Y\tan\alpha}{(Y^2+R_o^2+2R_oY\sin\theta)^{1/2}}\right] dY \qquad \text{(E-4)}$$

By integrating by parts, the integral $F_{12}$ becomes

$$F_{12} = -\frac{\sin\theta}{\pi}\tan^{-1}\left(\frac{B\tan\alpha}{c}\right) + \frac{1}{\pi}\left[\frac{Y_o\sin\theta + R_o}{(Y_o^2+R_o^2+2R_oY_o\sin\theta)^{1/2}}\right] \times$$

$$\tan^{-1}\left[\frac{(B/C)Y_o\tan\alpha}{(Y_o^2+R_o^2+2R_oY_o\sin\theta)^{1/2}}\right] + F_{13} \qquad \text{(E-5)}$$

where

$$F_{13} = \frac{1}{\pi}\int_{Y_o}^{\infty} \frac{(B/C)R_o \tan\alpha\,(Y\sin\theta + R_o)^2 \qquad dY}{(Y_o^2+R_o^2+2R_oY\sin\theta)[(R^2Y^2\sec^2\alpha/c^2)+R_o^2+2R_oY\sin\theta]} \tag{E-6}$$

The integrals $F_{11}$ and $F_{13}$ can be combined and simplified to become

$$F_{11} + F_{13} = \frac{1}{\pi}\int_{Y_o}^{\infty} \frac{(B/C)R_o \tan\alpha \qquad dY}{[R^2Y^2\sec^2\alpha/C^2+R_o^2+2R_oY\sin\theta]} \tag{E-7}$$

or, by direct integration,

$$F_{11} + F_{13} = \frac{B\tan\alpha}{2\sqrt{R^2+B^2\tan^2\alpha}} - \frac{B\tan\alpha}{\pi\sqrt{R^2+B^2\tan^2\alpha}}$$

$$\times \tan^{-1}\left[\frac{(R^3/B^2C)\sec^2\alpha\, Y_o - (1-H\tan\alpha)\tan\alpha}{\sqrt{R^2 + B^2\tan^2\alpha}}\right] \tag{E-8}$$

where $\theta$ and $R_o$ have been eliminated by use of relations in Eqs. (43) and (47).

The results in Eqs. (E-5) and (E-8) with $Y_o$ given by Eq. (52) give the configuration factor for the tangent region as

$$F_1 = \frac{1}{\pi C}[(1-H\tan\alpha)\tan\alpha]\tan^{-1}\left(\frac{B\tan\alpha}{C}\right) - \frac{1}{\pi M}[R^2-\bar{H}\tan\alpha(1-H\tan\alpha)$$

$$-2(1-H\tan\alpha)^2]\tan^{-1}\left\{\frac{B}{M}[(1-H\tan\alpha)+\tan\alpha\bar{\bar{H}}]\right\} + \frac{B\tan\alpha}{2\sqrt{R^2+B^2\tan^2\alpha}} - \frac{B\tan\alpha}{\pi\sqrt{R^2+B^2\tan^2\alpha}}$$

$$\times \tan^{-1}\left\{\frac{(R^2/B^2)\sec^2\alpha\,\bar{H} - (1-H\tan\alpha)[1-(R^2/B^2)\operatorname{cosec}^2\alpha]\tan\alpha}{\sqrt{R^2 + B^2\tan^2\alpha}}\right\}$$

where

$$M = \sqrt{\{\bar{H}+[(1-H\tan\alpha)/\tan\alpha]\}^2 \; R^2 + [(1-H\tan\alpha)\tan\alpha \; \bar{H}-R^2+2(1-H\tan\alpha)^2]^2} \tag{56}$$

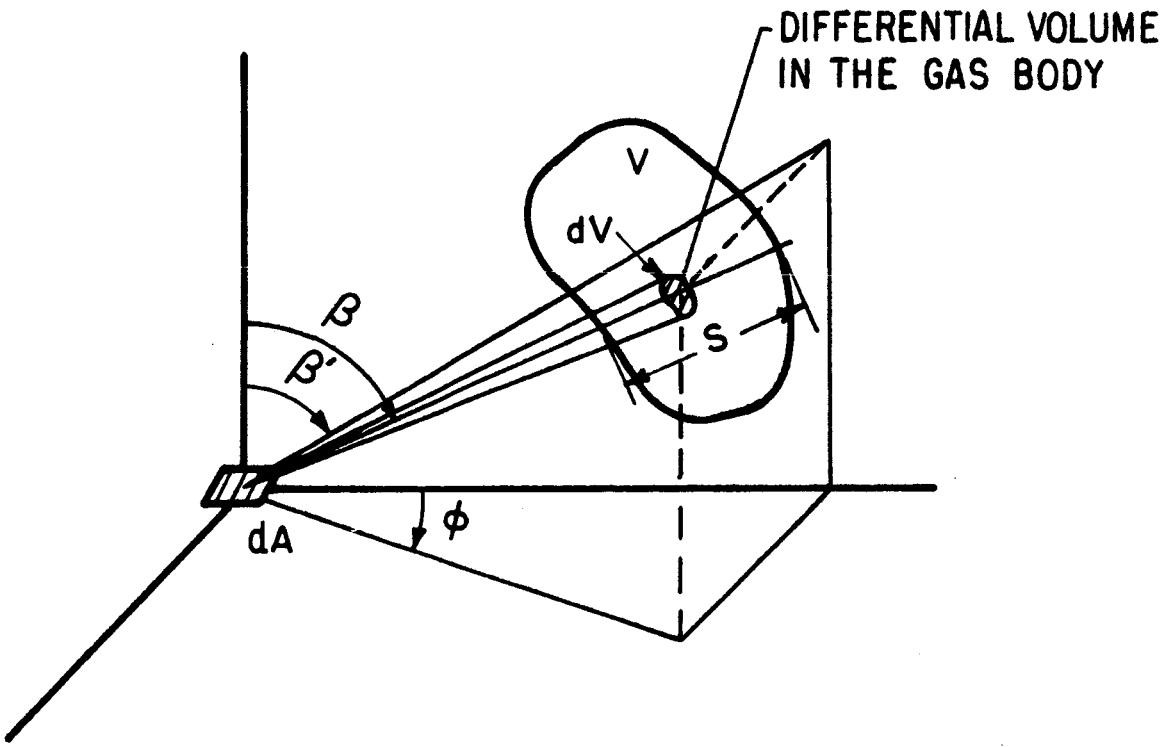


FIG. 1 RADIATION FROM A GAS BODY

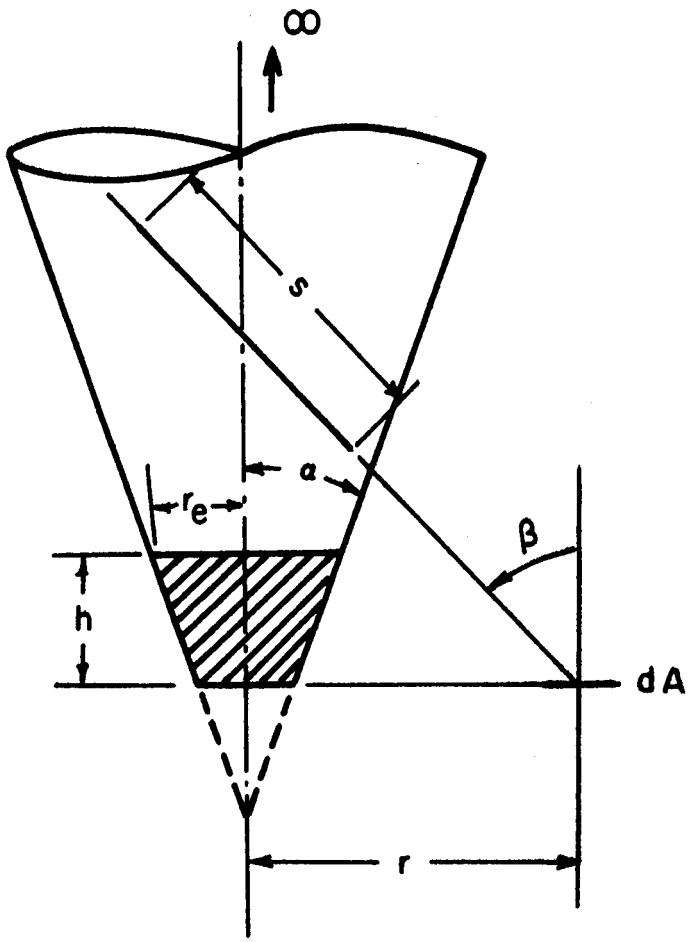


FIG. 2 THE CONICAL GAS BODY

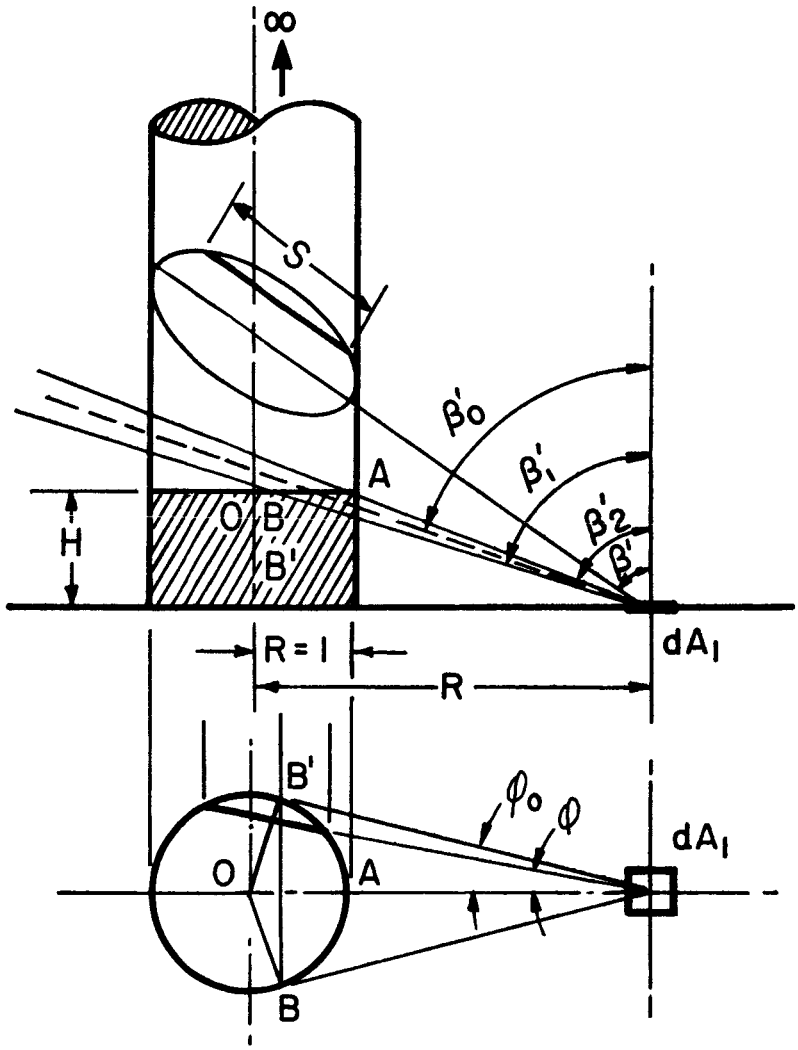


FIG. 3 THE SEMI-INFINITE CYLINDRICAL GAS BODY

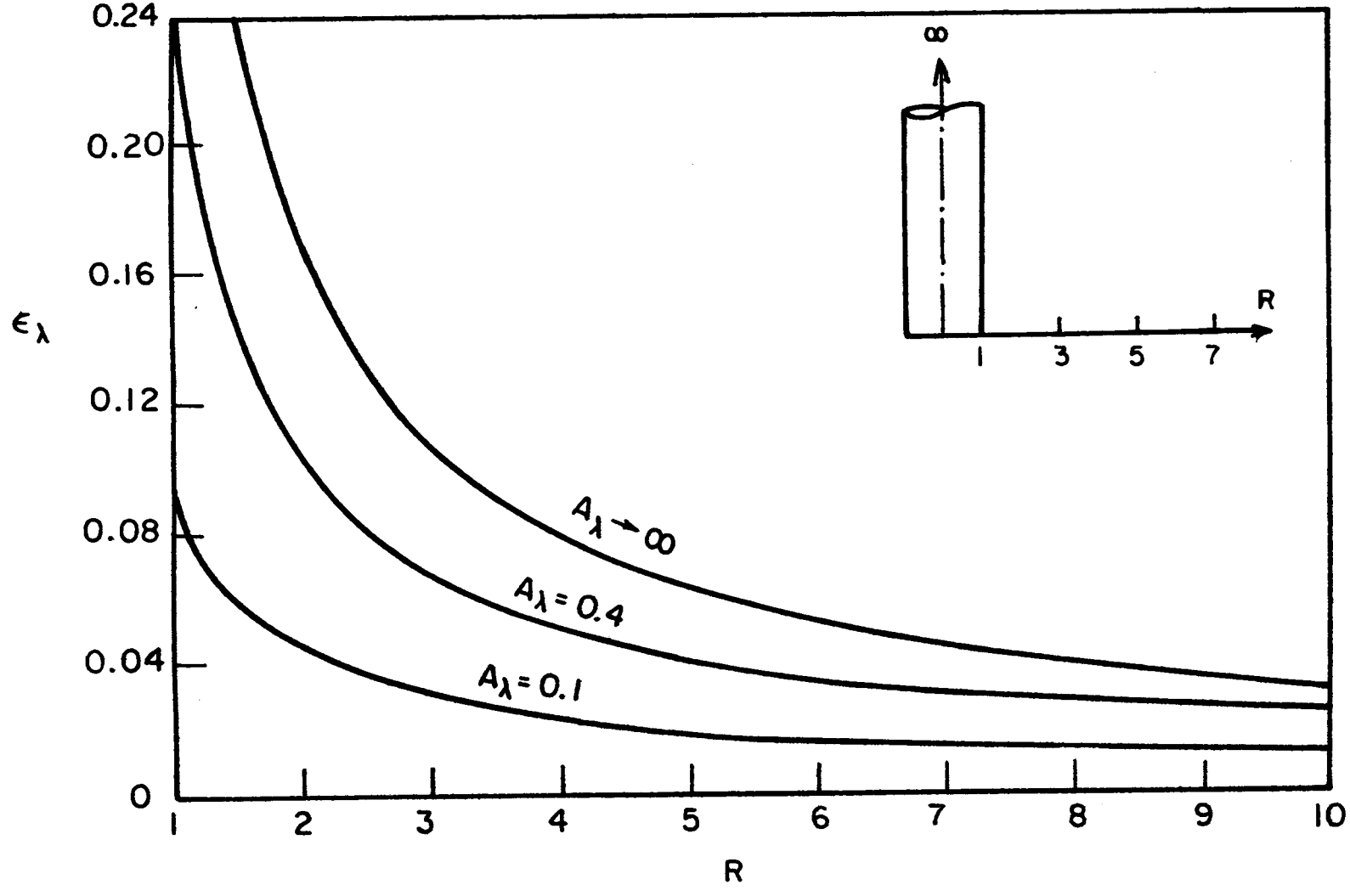


FIG. 4 SPECTRAL APPARENT EMISSIVITY IN THE BASE PLANE OF A CYLINDRICAL GAS BODY (H=0)

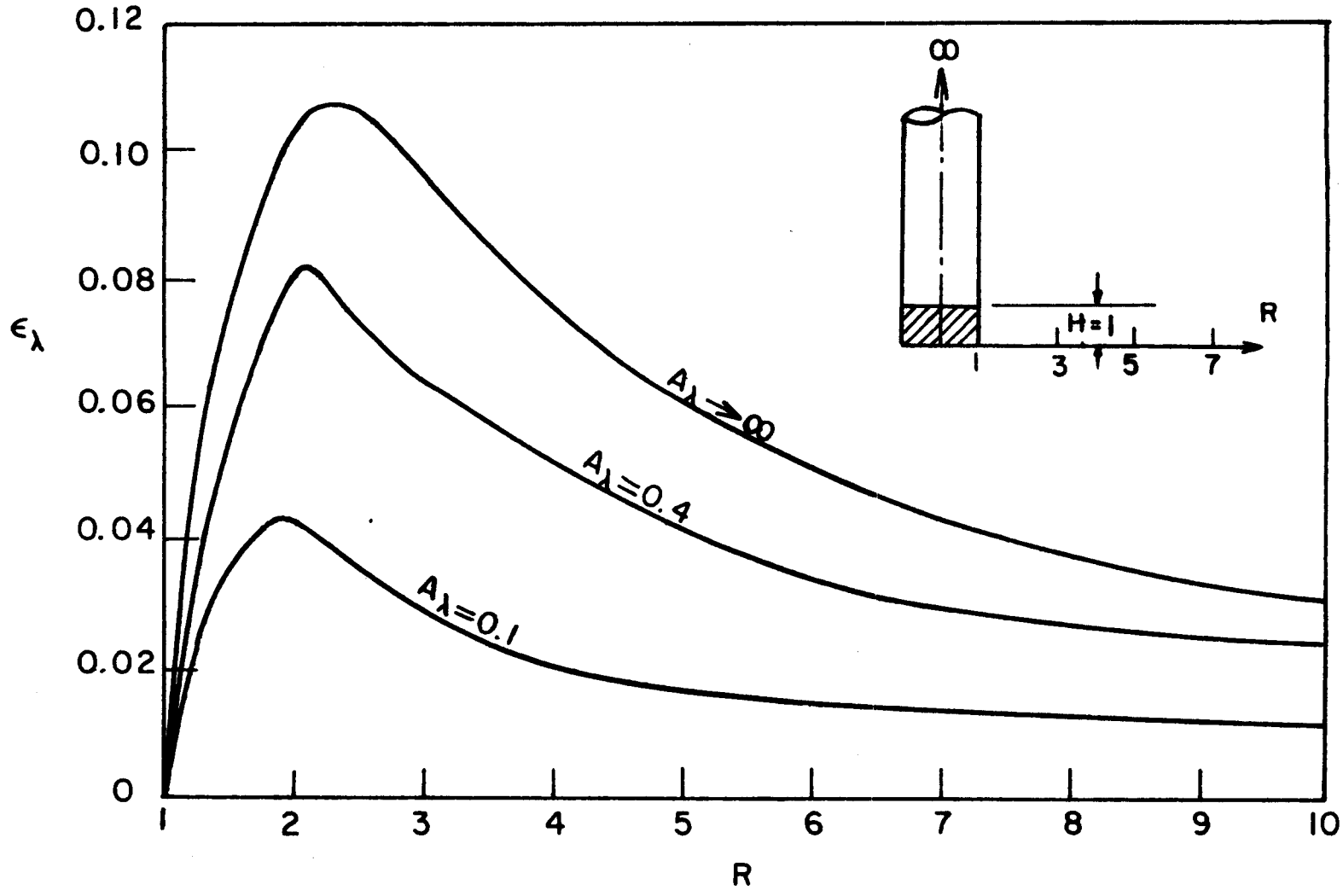


FIG. 5 SPECTRAL APPARENT EMISSIVITY IN THE BASE PLANE OF A CYLINDRICAL GAS BODY (H = 1)



HYD 8021

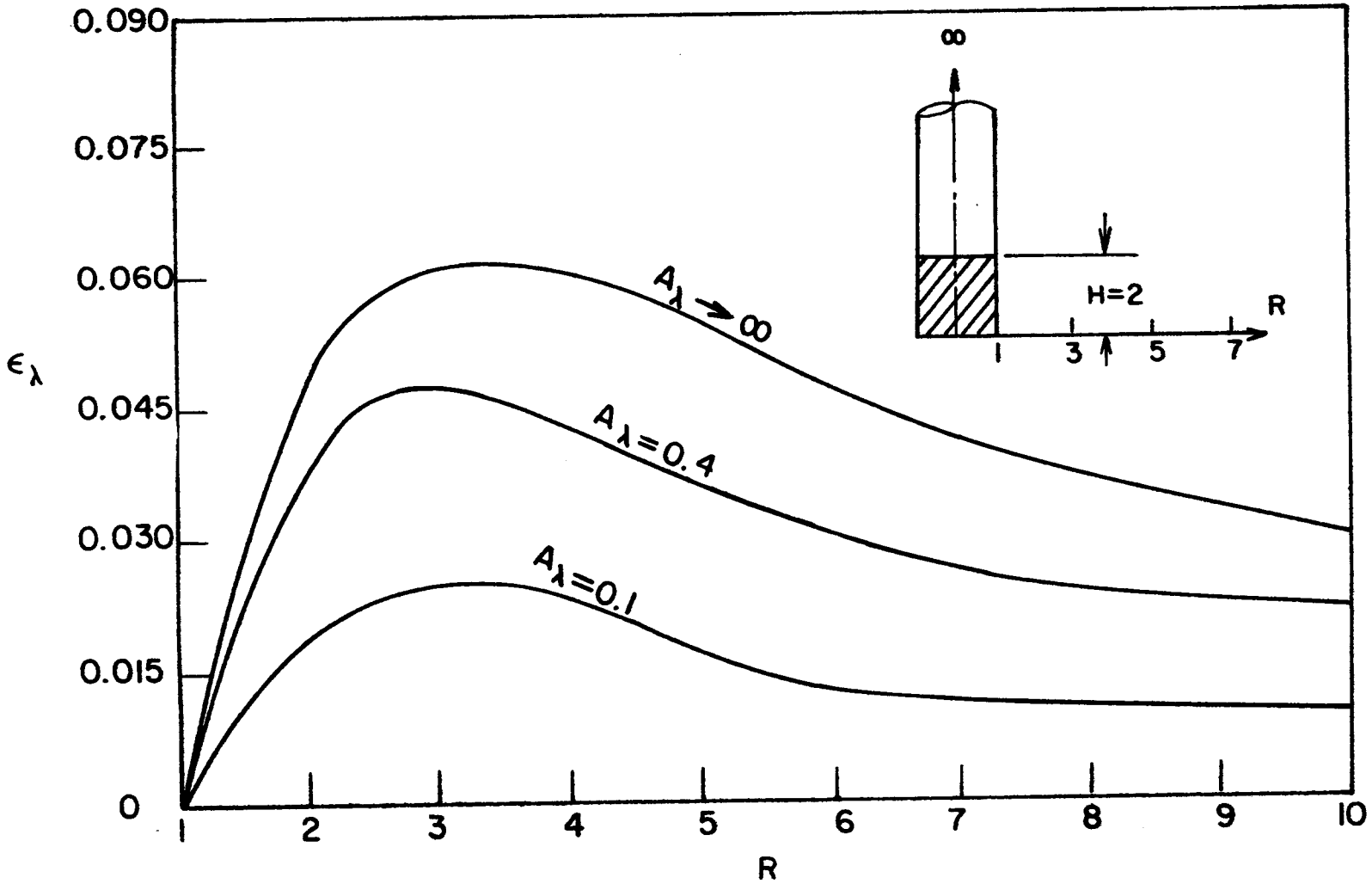


FIG. 6 SPECTRAL APPARENT EMISSIVITY IN THE BASE PLANE OF A CYLINDRICAL GAS BODY (H=2)

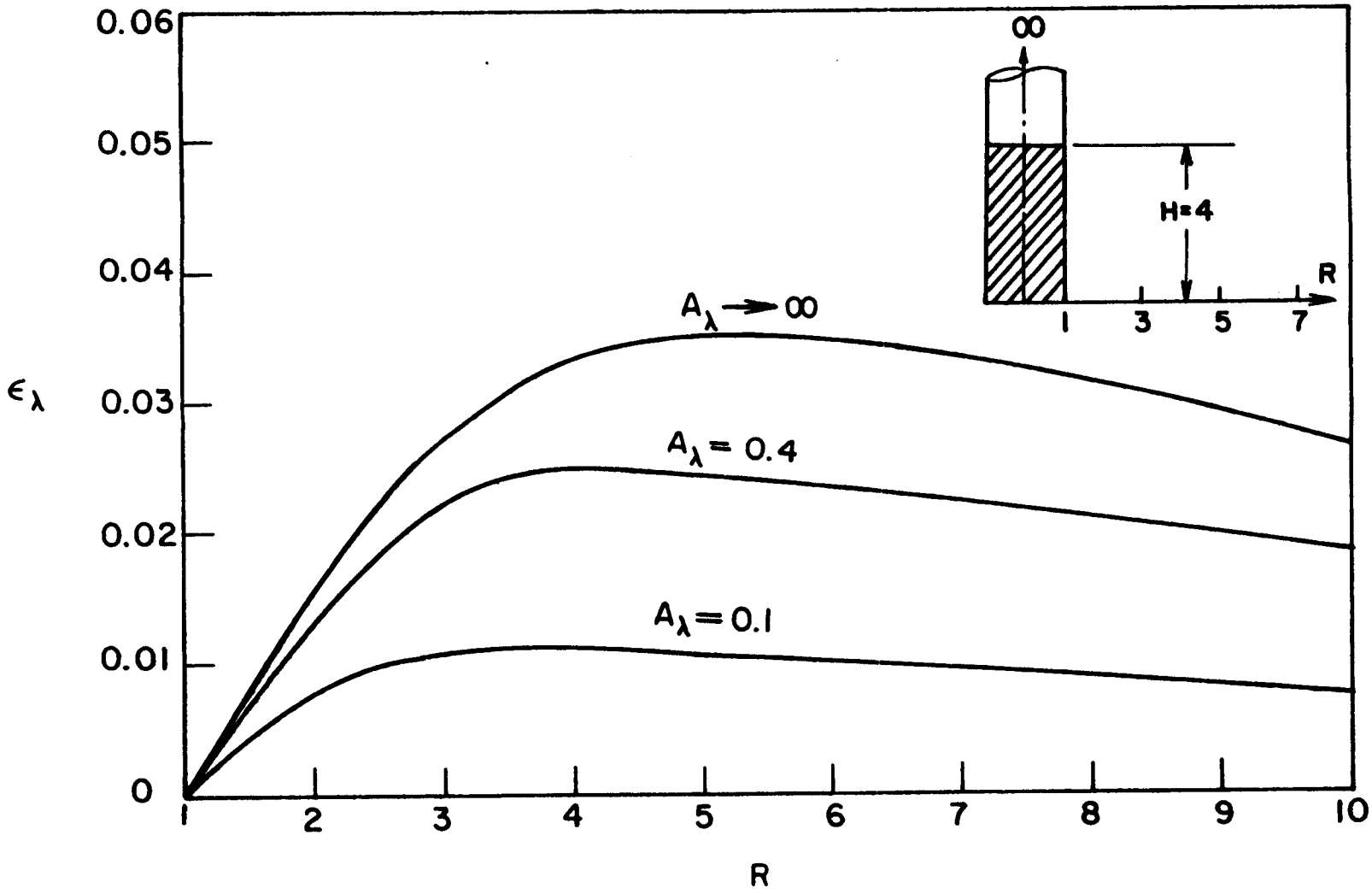


FIG. 7 SPECTRAL APPARENT EMISSIVITY IN THE BASE PLANE OF A CYLINDRICAL GAS BODY (H=4)

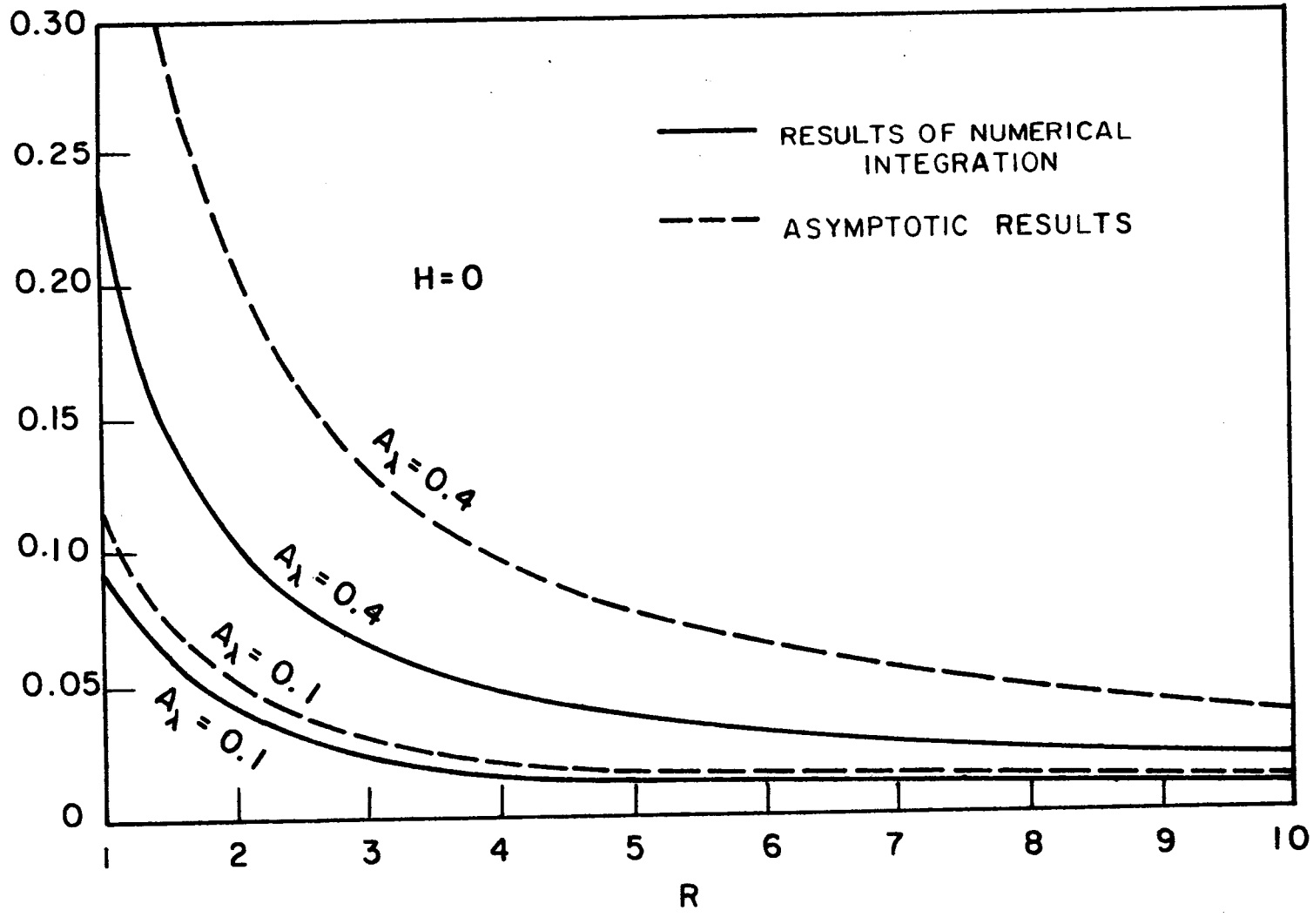


FIG. 8 COMPARISON BETWEEN RESULTS FROM ASYMPTOTIC EXPRESSION FOR $A_\lambda \ll 1$, H=0, AND RESULTS OF NUMERICAL INTEGRATION FOR A CYLINDRICAL GAS BODY

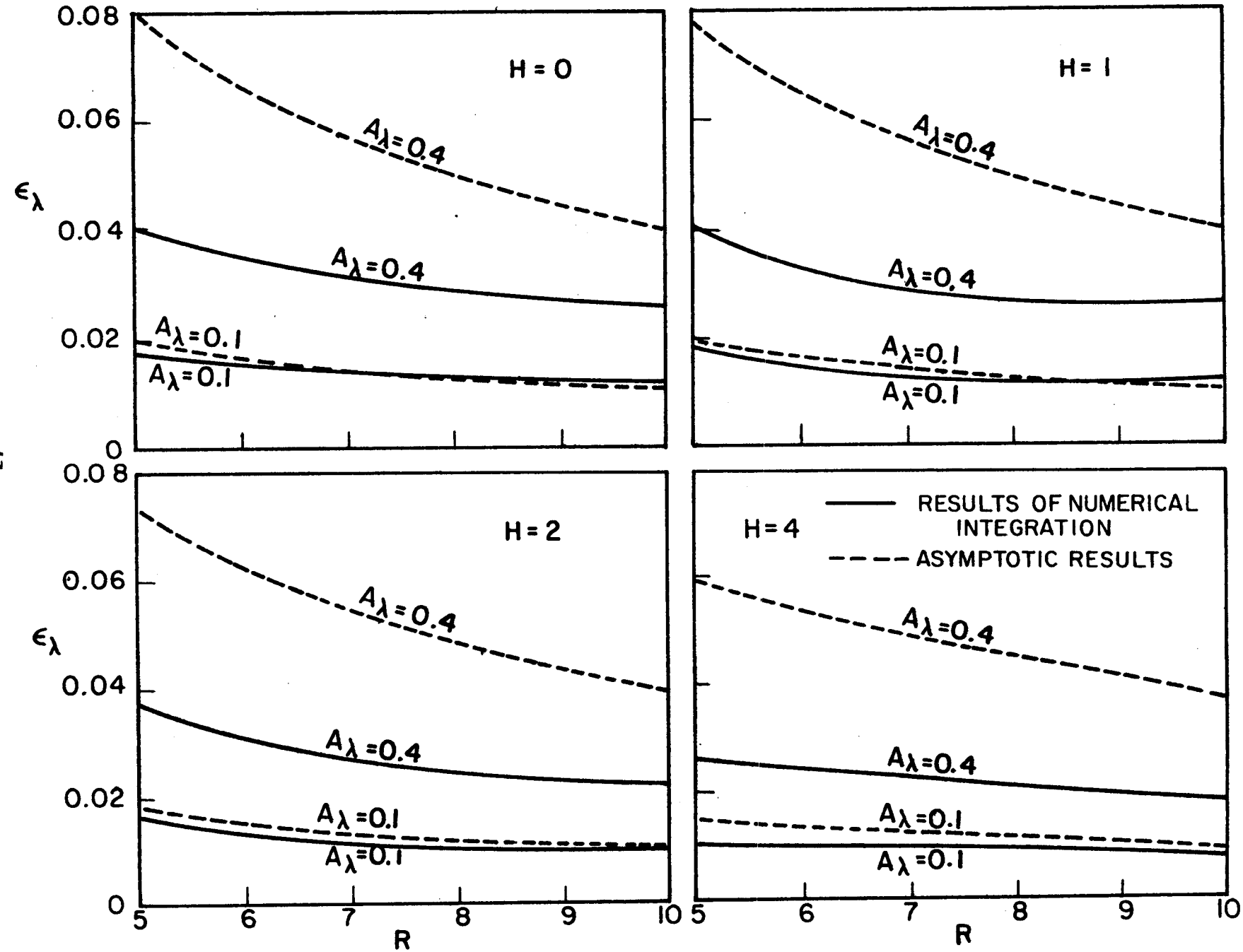


FIG. 9 COMPARISON BETWEEN RESULTS FROM ASYMPTOTIC EXPRESSON FOR $A_\lambda \ll 1$, $R \gg 1$, AND RESULTS OF NUMERICAL INTEGRATION FOR A CYLINDRICAL GAS BODY

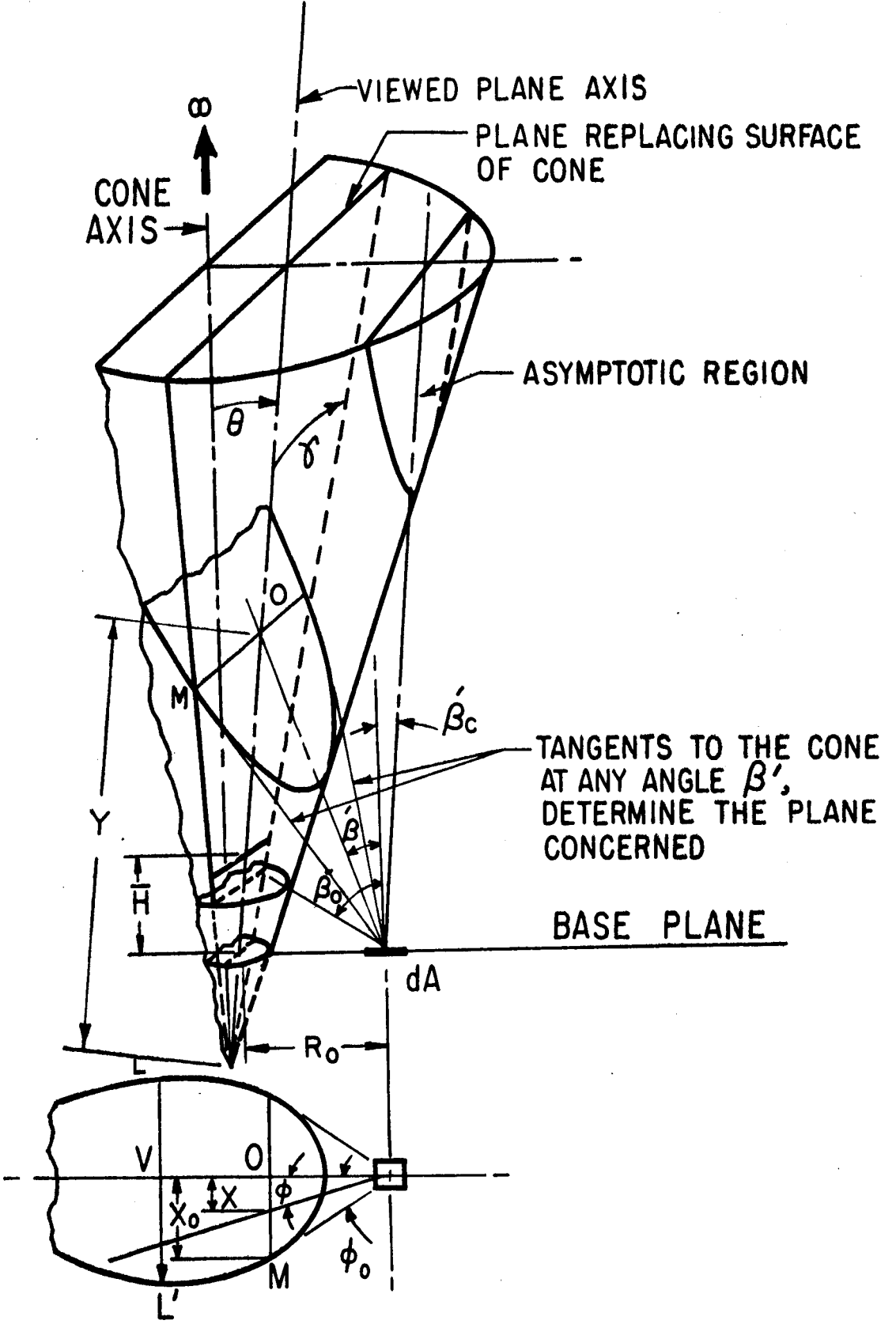


FIG. 10 GEOMETRICAL DIAGRAM OF A CONICAL GAS BODY

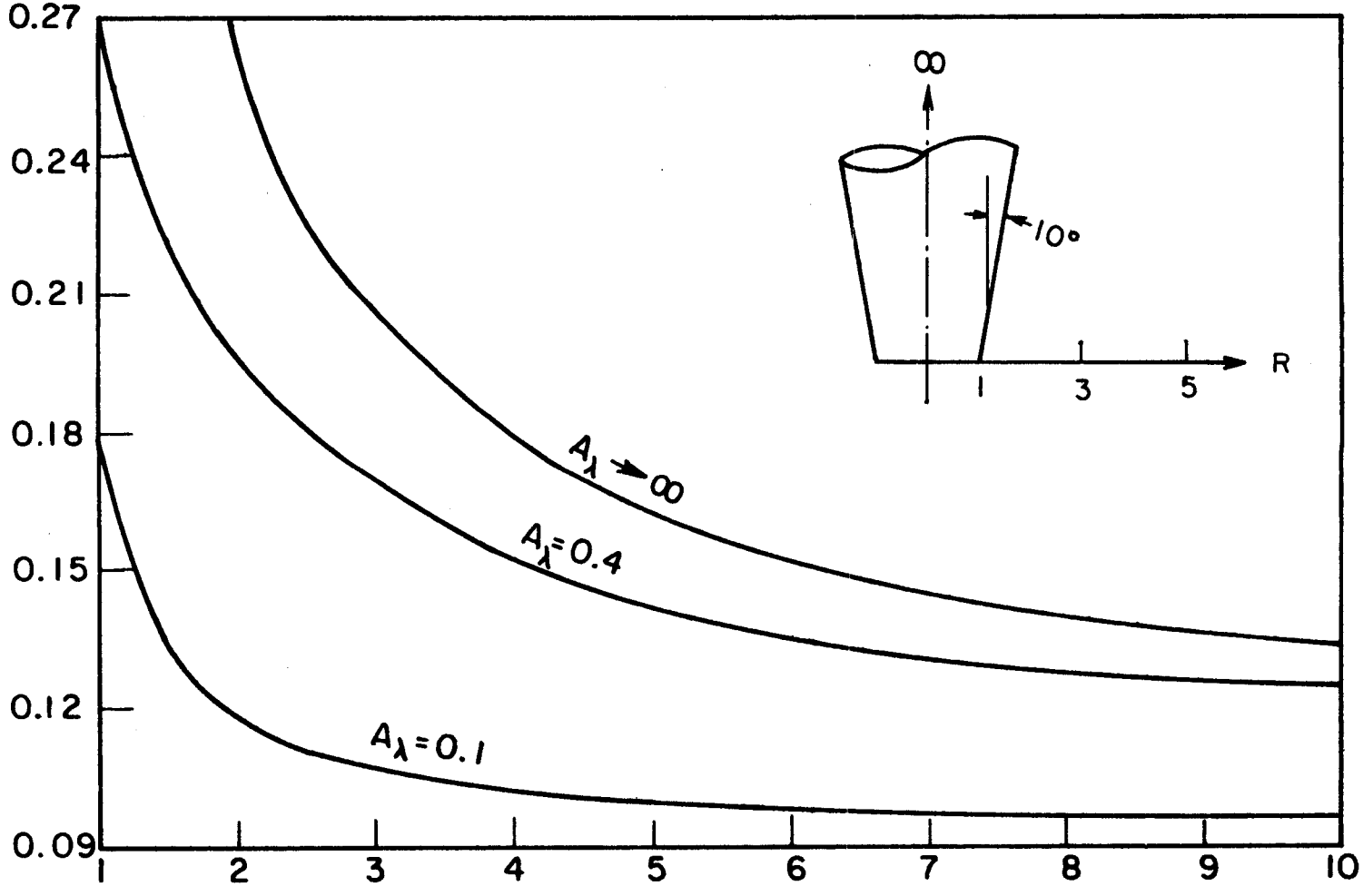


FIG. 11 SPECTRAL APPARENT EMISSIVITY IN THE BASE PLANE OF A CONICAL GAS BODY ( $\alpha = 10°$, $H = 0$ )

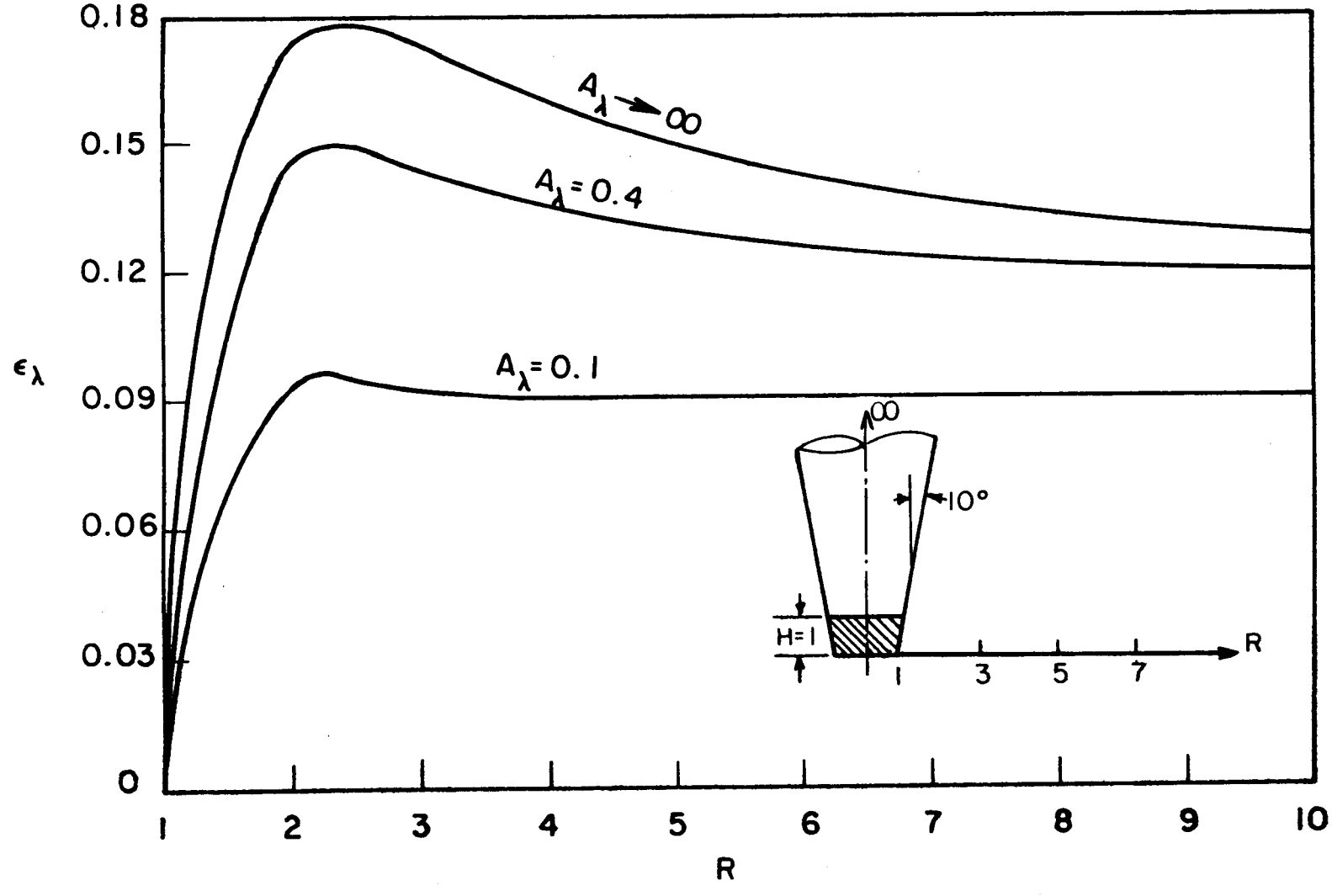


FIG.12 SPECTRAL APPARENT EMISSIVITY IN THE BASE PLANE OF A CONICAL GAS BODY ( $\alpha = 10°$, H = 1)

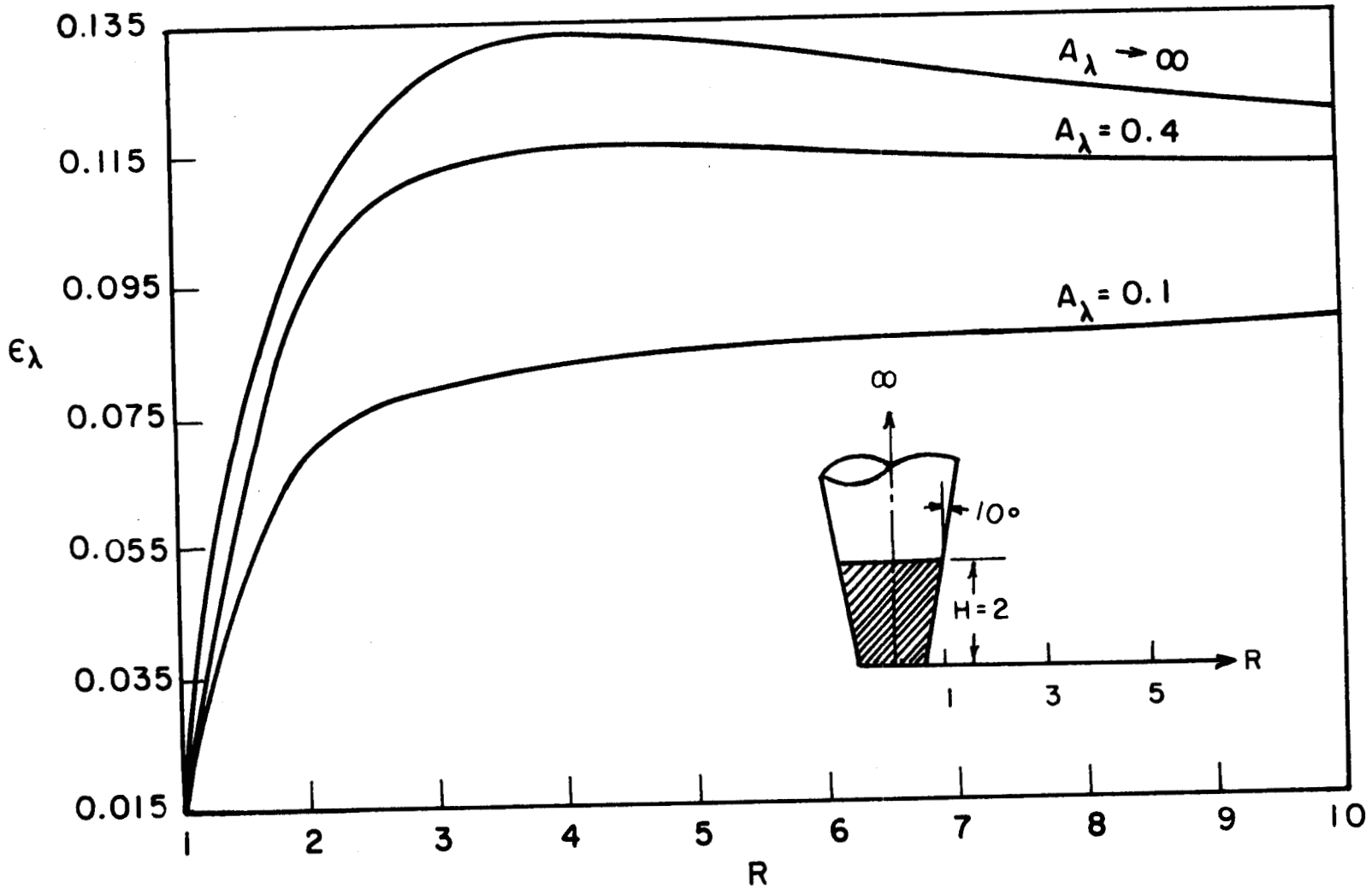


FIG. 13 SPECTRAL APPARENT EMISSIVITY IN THE BASE PLANE OF A CONICAL GAS BODY ($\alpha = 10°$, $H = 2$)

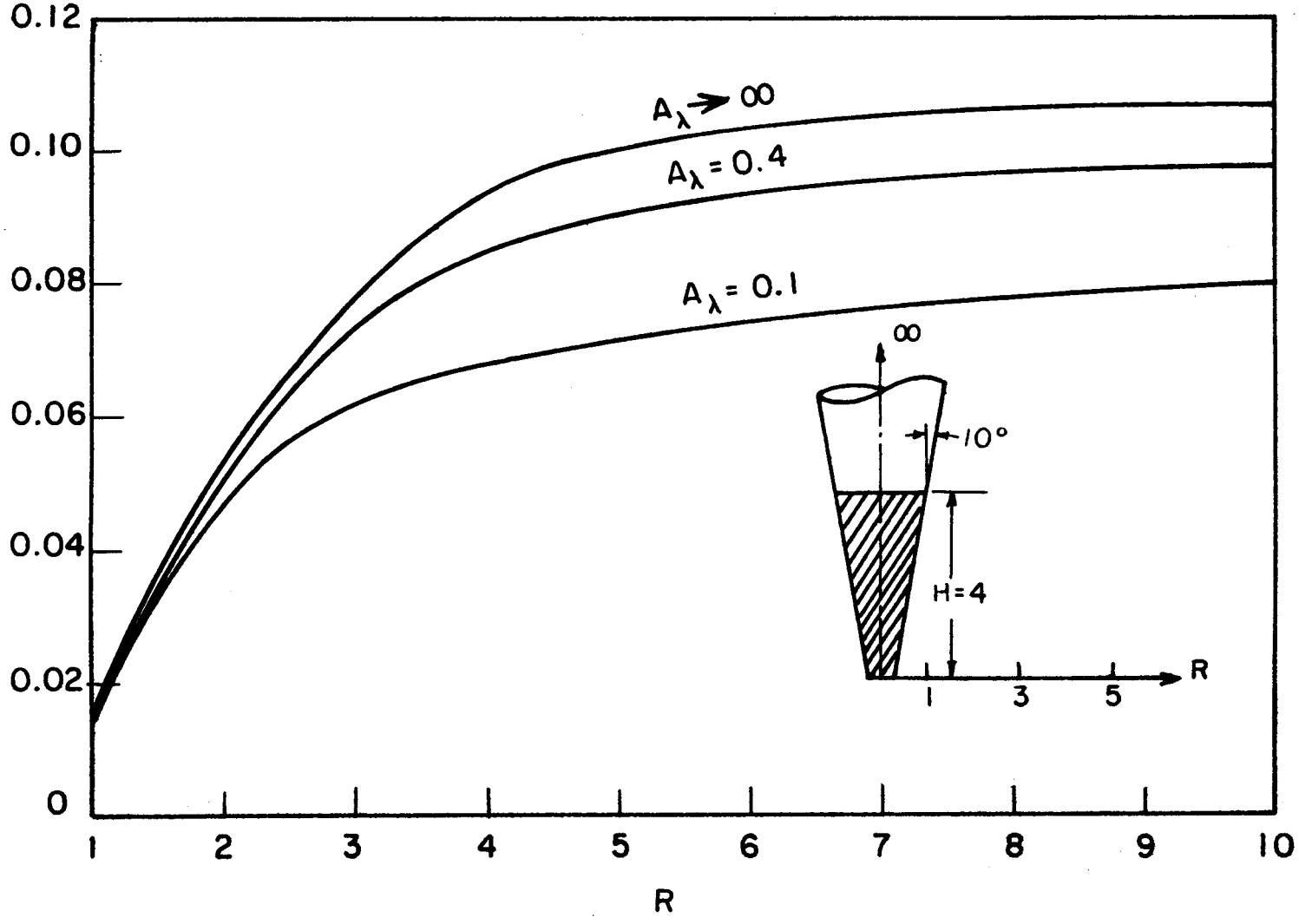


FIG. 14 SPECTRAL APPARENT EMISSIVITY IN THE BASE PLANE OF A CONICAL GAS BODY ( $\alpha = 10°$, H=4)

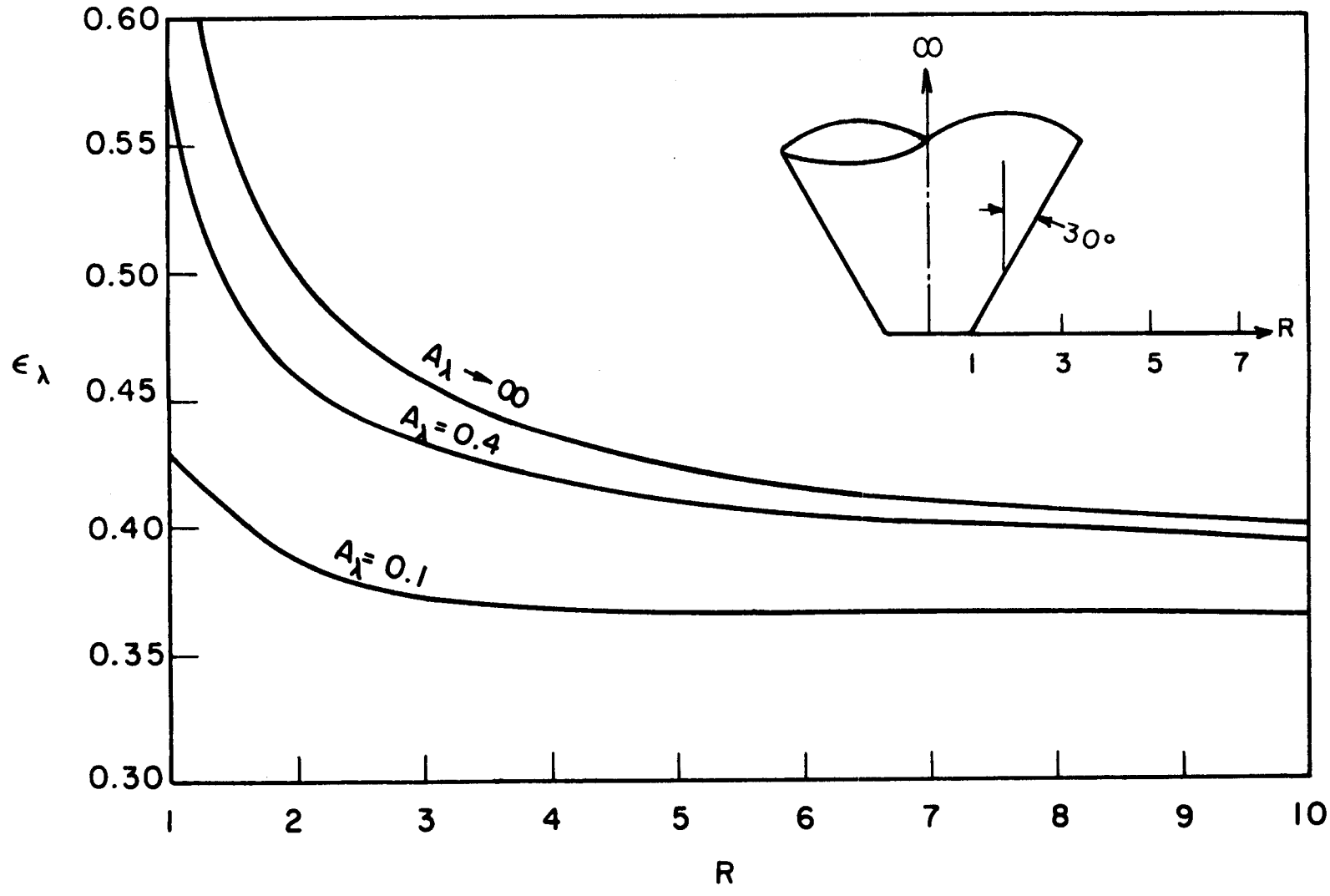


FIG. 15 SPECTRAL APPARENT EMISSIVITY IN THE BASE PLANE OF A CONICAL GAS BODY ( $\alpha$ =30°, H = 0)

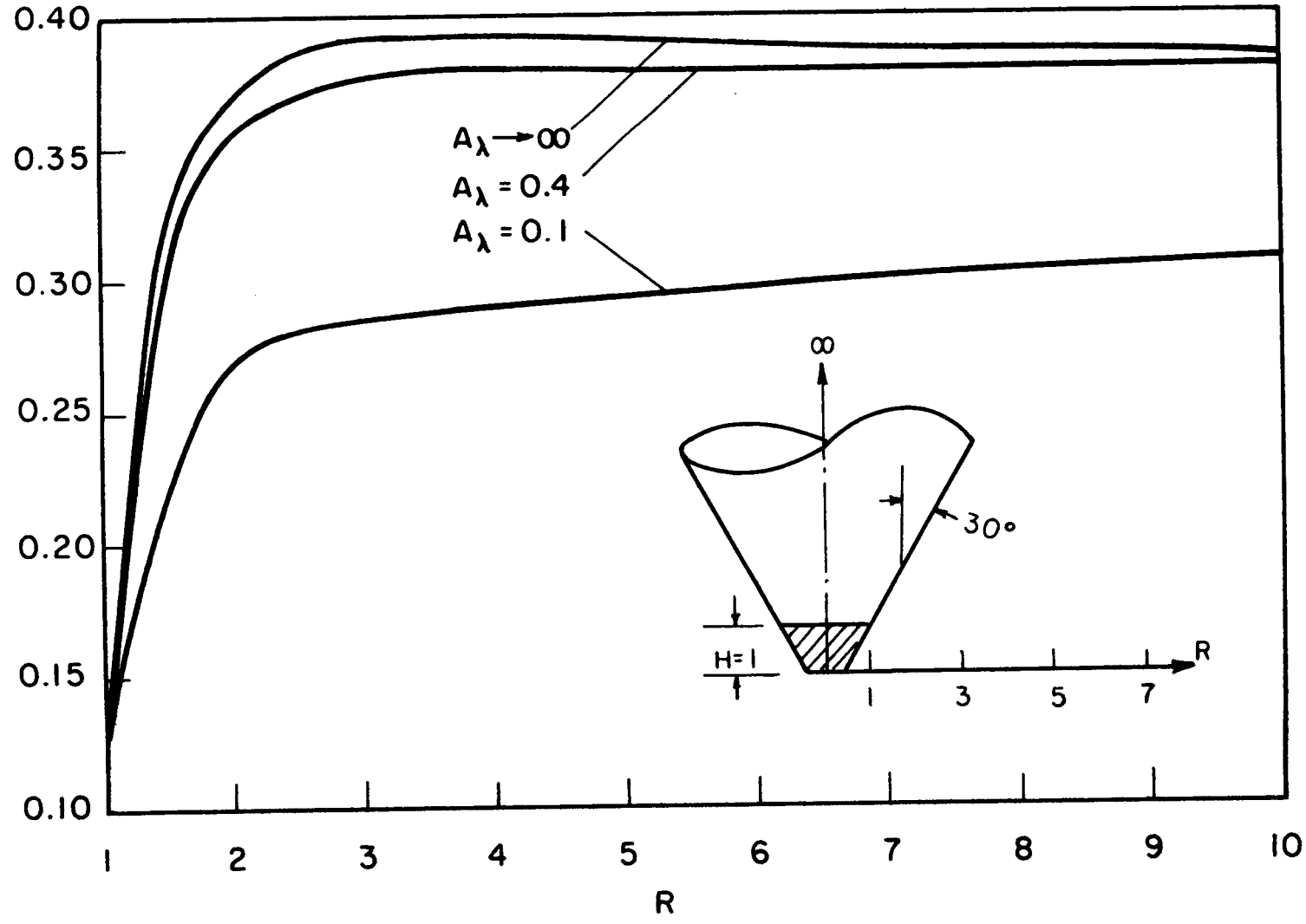


FIG. 16 SPECTRAL APPARENT EMISSIVITY IN THE BASE PLANE OF A CONICAL GAS BODY ( $\alpha = 30°$, $H = 1$ )

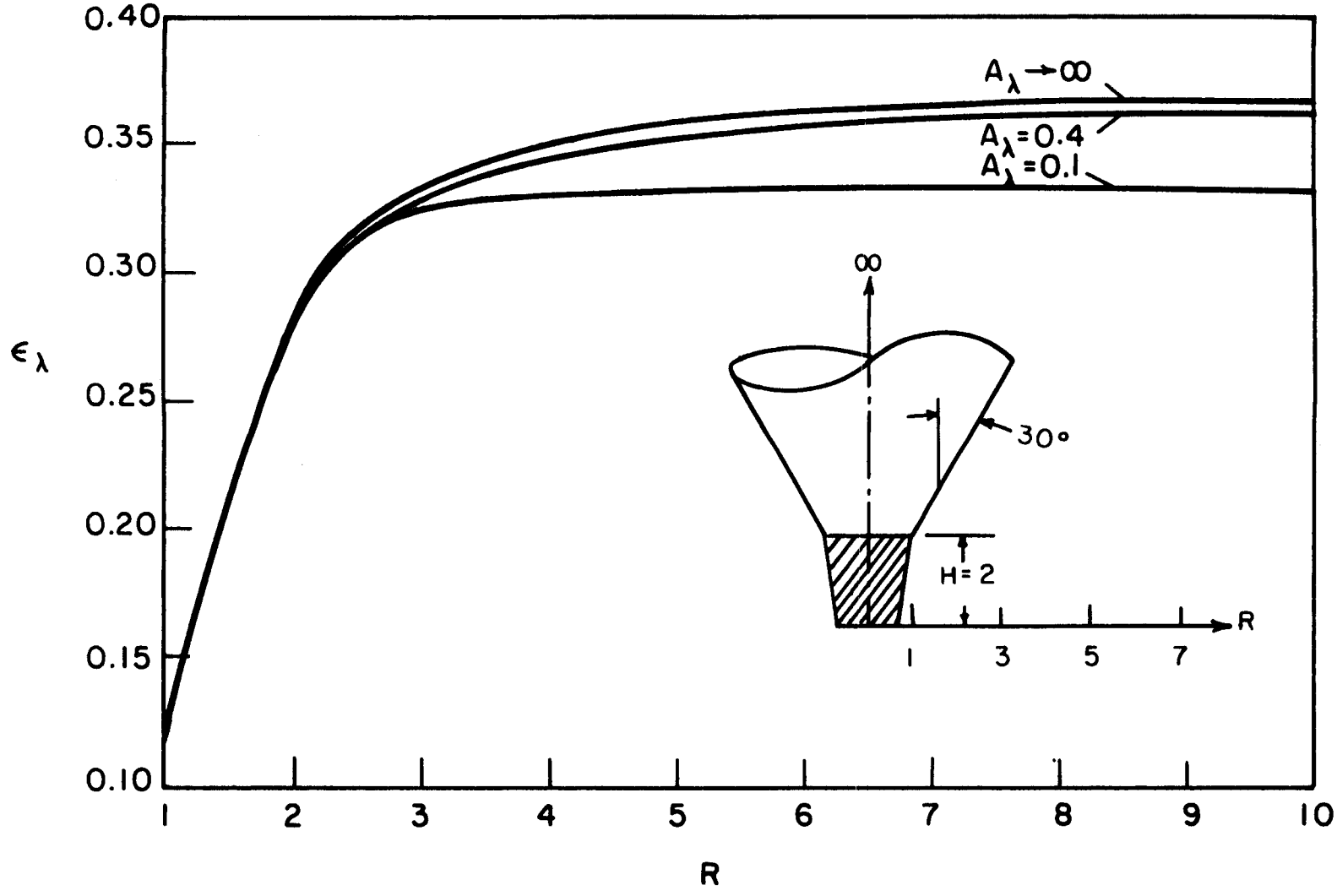


FIG. 17 SPECTRAL APPARENT EMISSIVITY IN THE BASE PLANE OF A CONICAL GAS BODY ( $\alpha = 30°$, $H = 2$)

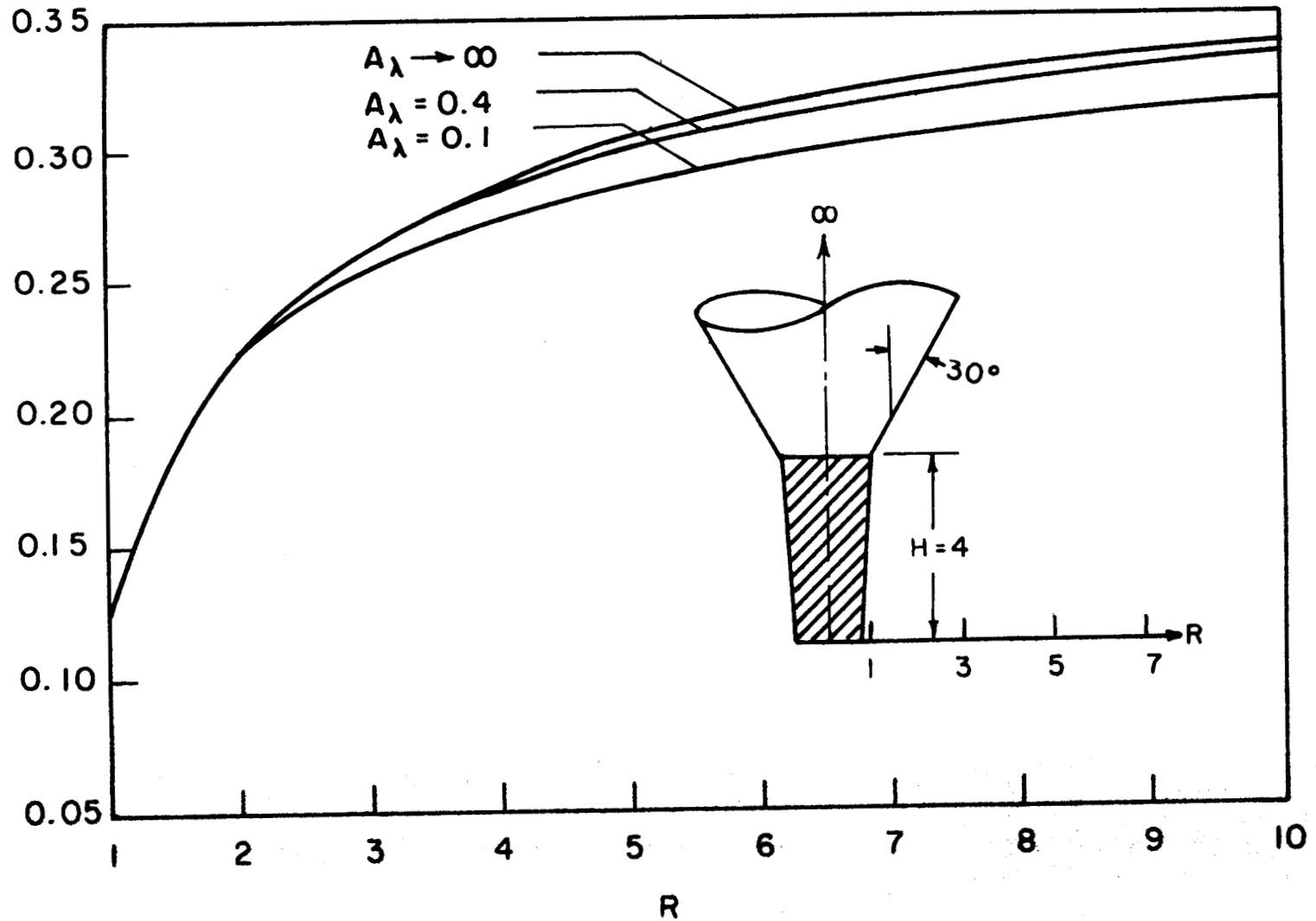


FIG. 18 SPECTRAL APPARENT EMISSIVITY IN THE BASE PLANE OF A CONICAL GAS BODY ( $\alpha = 30°$, $H = 4$ )

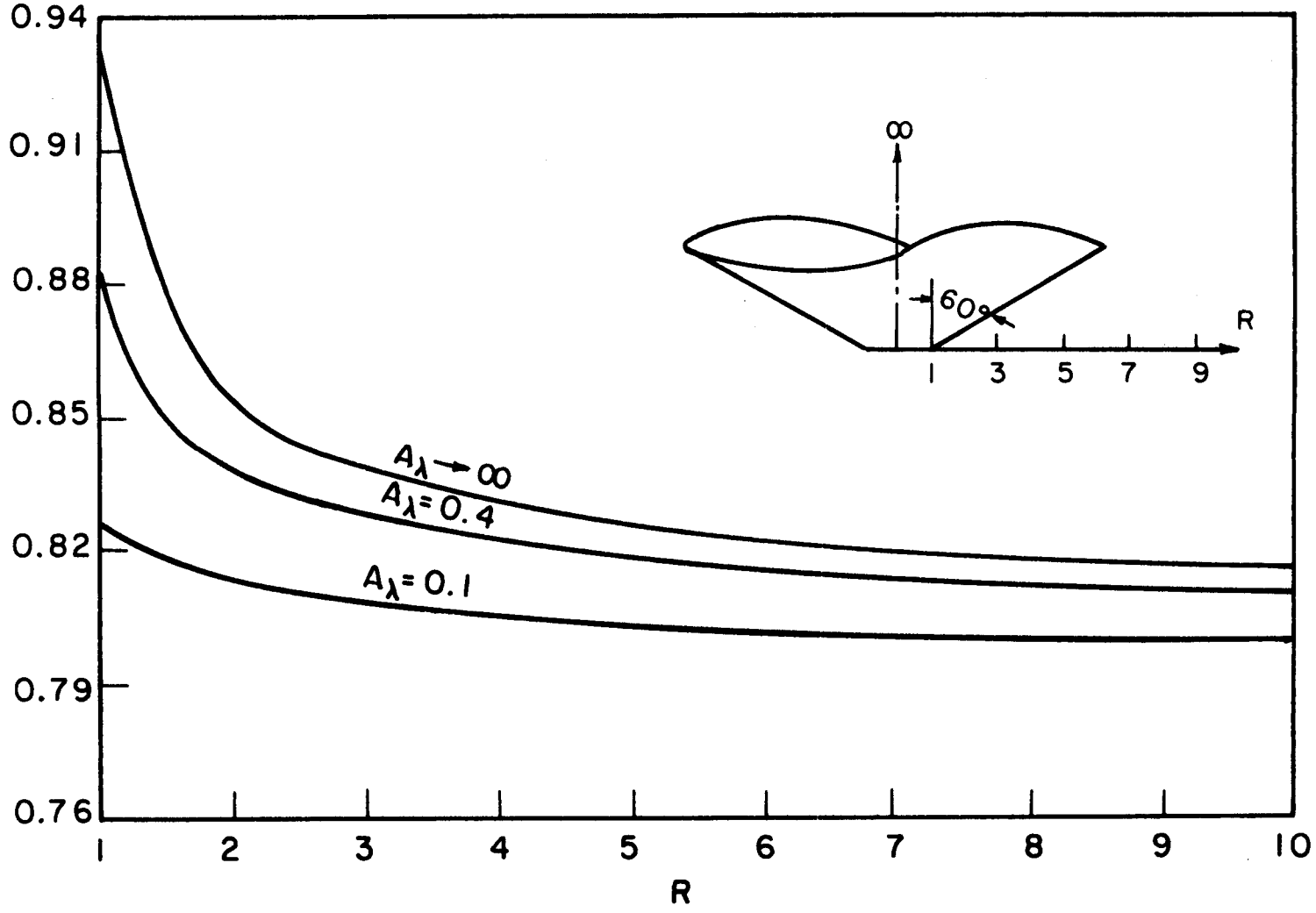


FIG. 19 SPECTRAL APPARENT EMISSIVITY IN THE BASE PLANE OF A CONICAL GAS BODY ($\alpha = 60°$, $H = 0$)

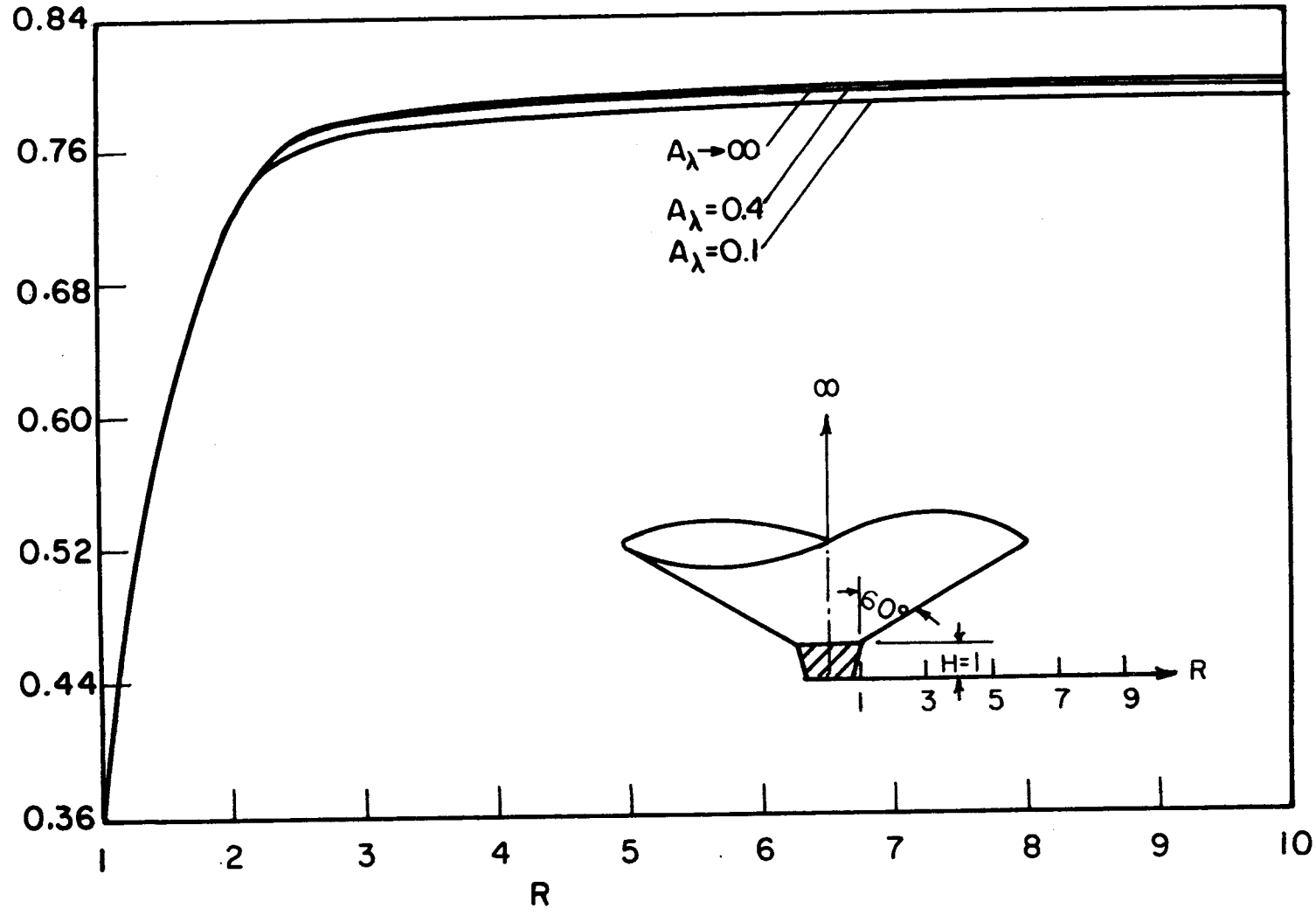


FIG. 20 SPECTRAL APPARENT EMISSIVITY IN THE BASE PLANE OF A CONICAL GAS BODY ( $\alpha = 60°$, $H = 1$ )

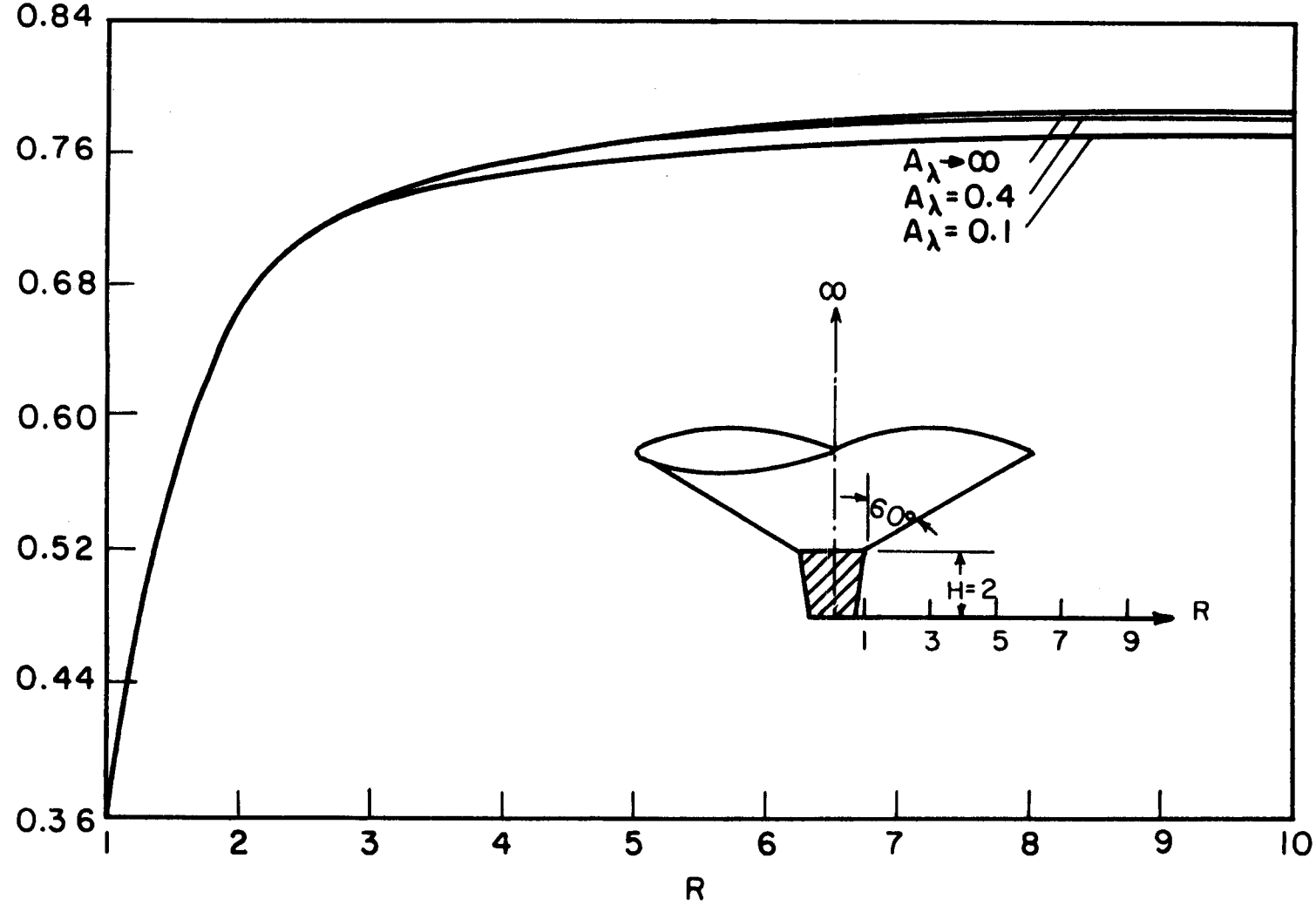


FIG. 21 SPECTRAL APPARENT EMISSIVITY IN THE BASE PLANE OF A CONICAL GAS BODY ( $\alpha = 60°$, H = 2)



HMD 8037

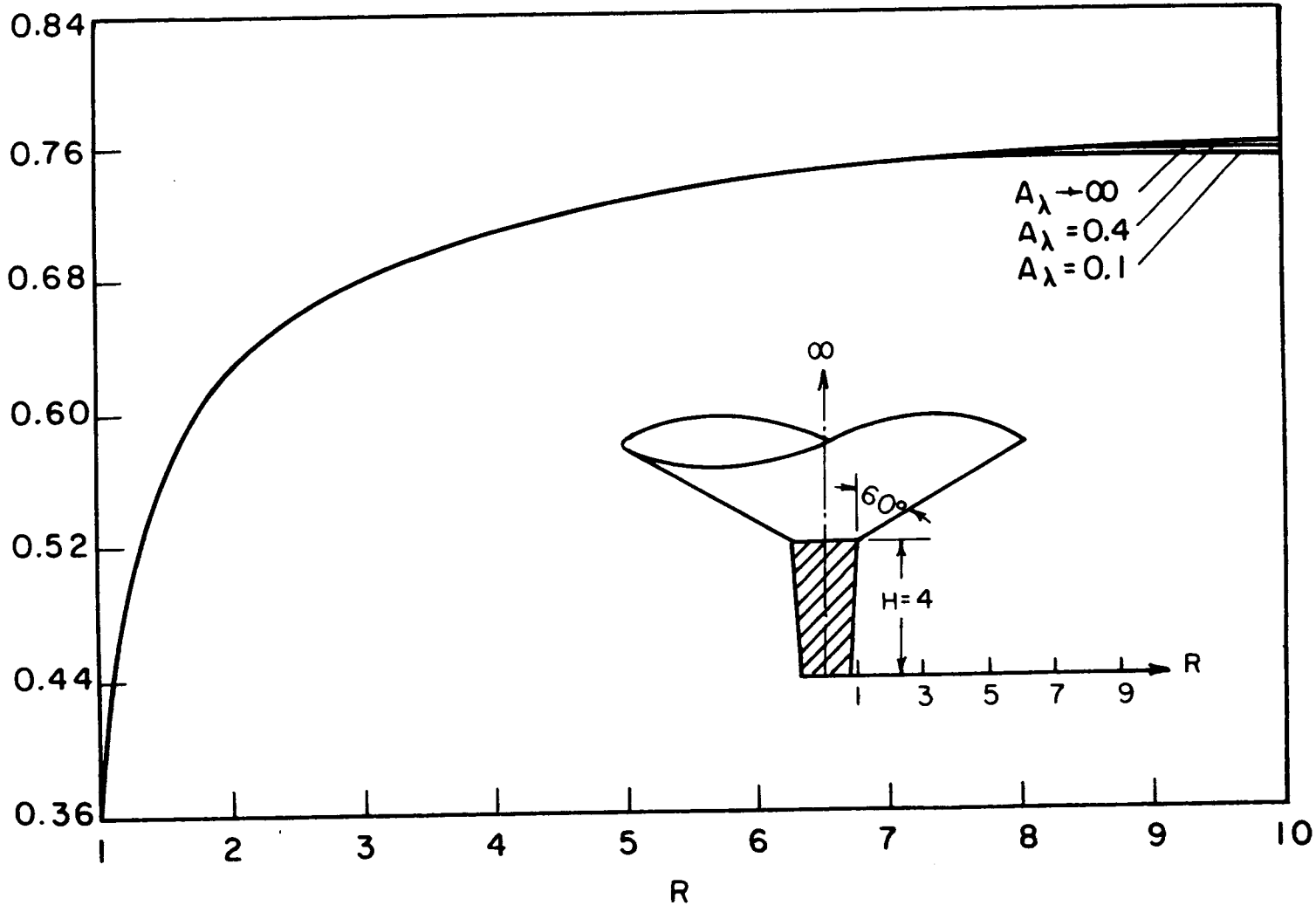


FIG. 22 SPECTRAL APPARENT EMISSIVITY IN THE BASE PLANE OF A CONICAL GAS BODY ( $\alpha = 60°$, H = 4 )

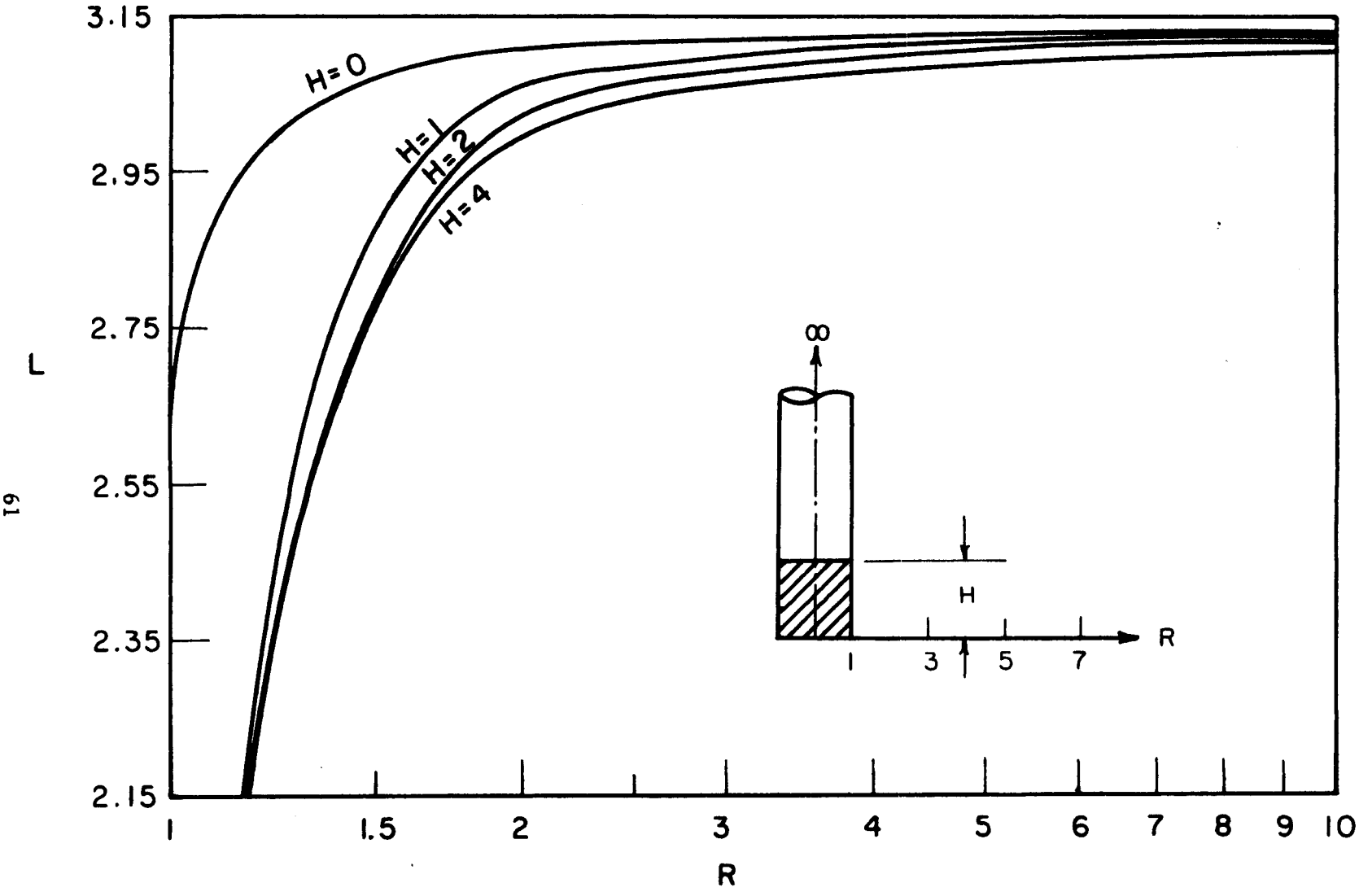


FIG. 23 DIMENSIONLESS MEAN PATH LENGTH FOR THE CYLINDRICAL GAS BODY

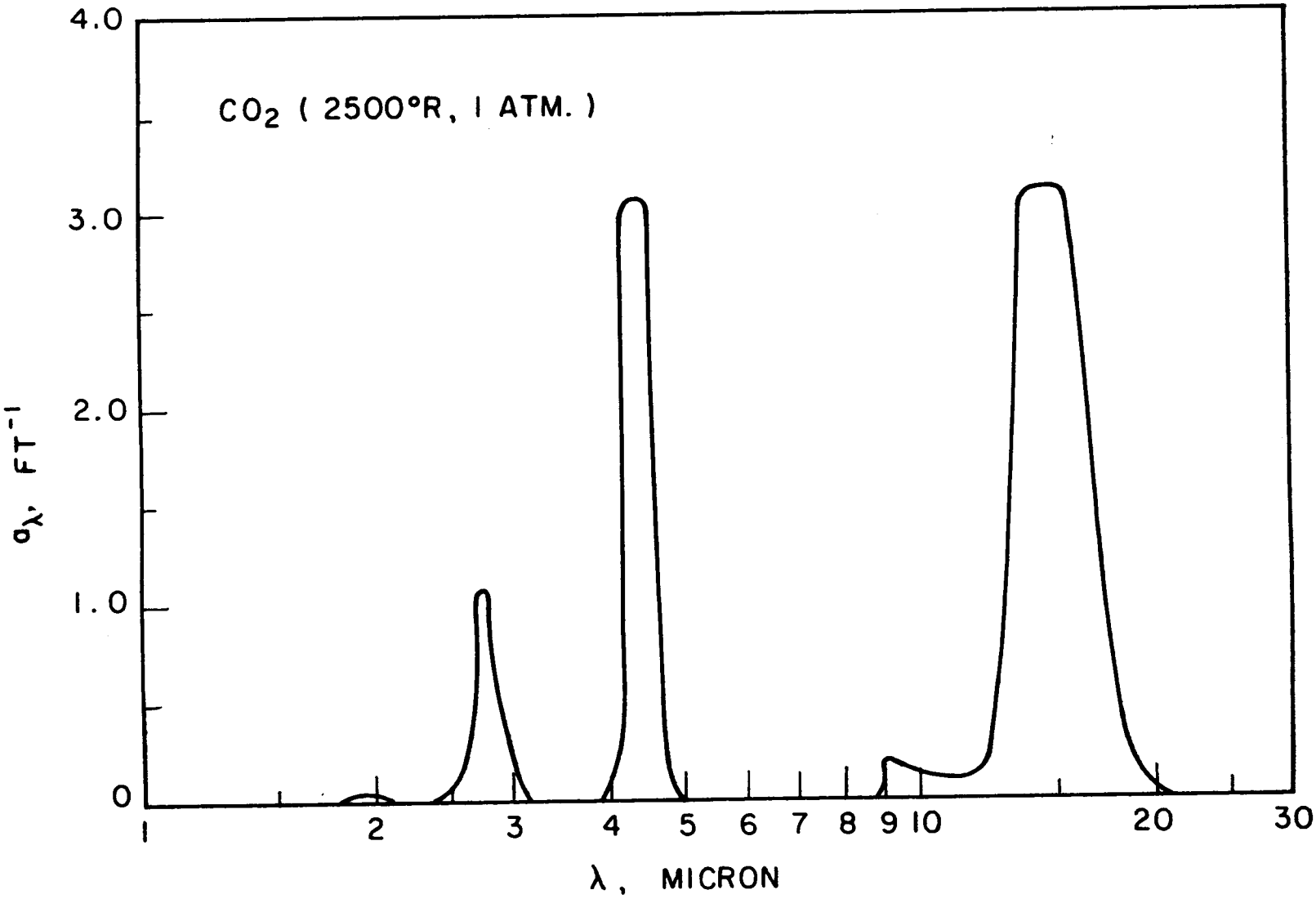


FIG.24 INFRARED ABSORPTION SPECTRUM OF $CO_2$ AT 2500°R AND I ATM.

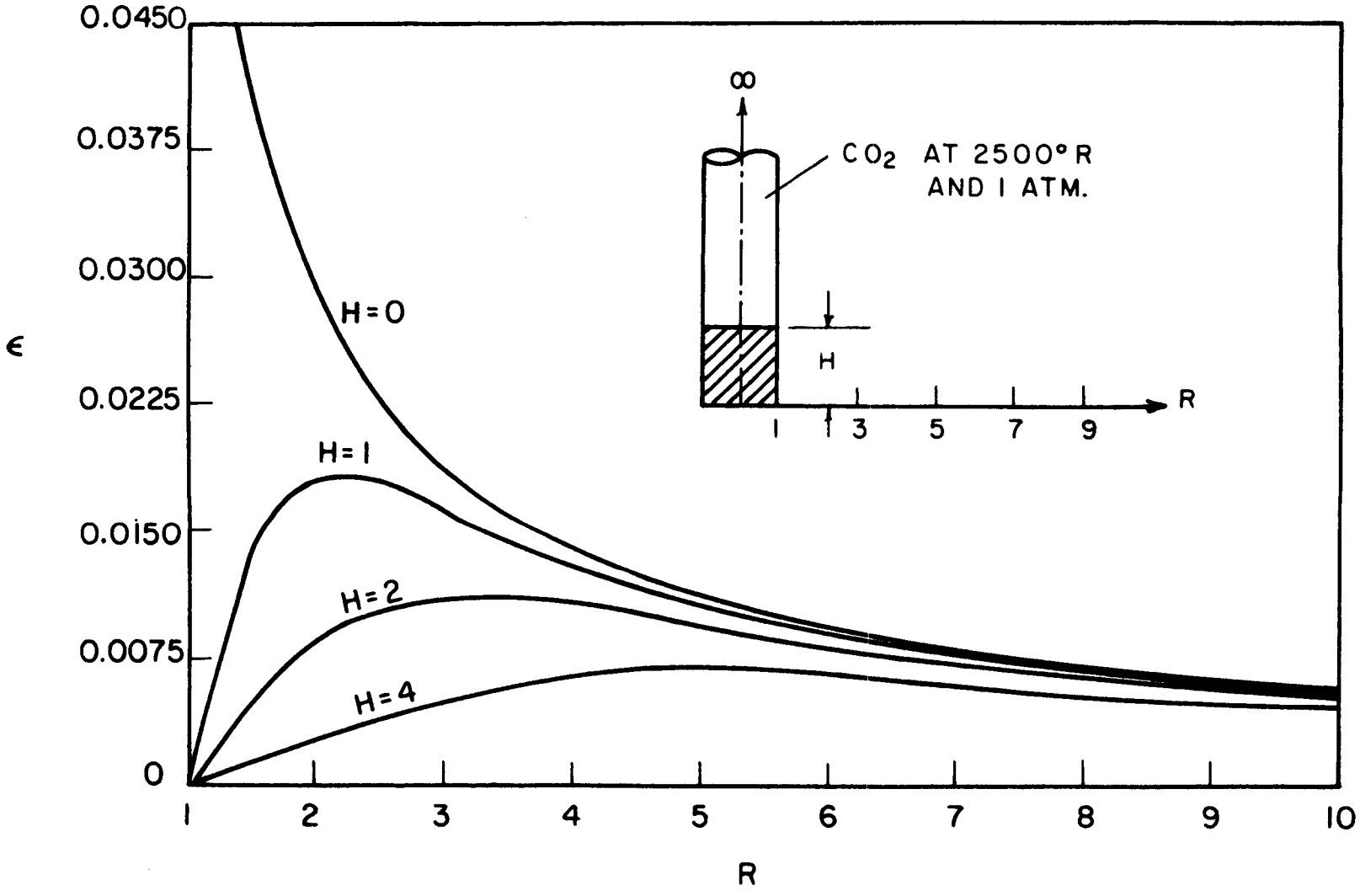


FIG. 25 APPARENT EMISSIVITIES IN THE BASE PLANE OF A SEMI-INFINITE CYLINDER OF CARBON DIOXIDE AT 2500 °R AND ONE ATMOSPHERIC PRESSURE

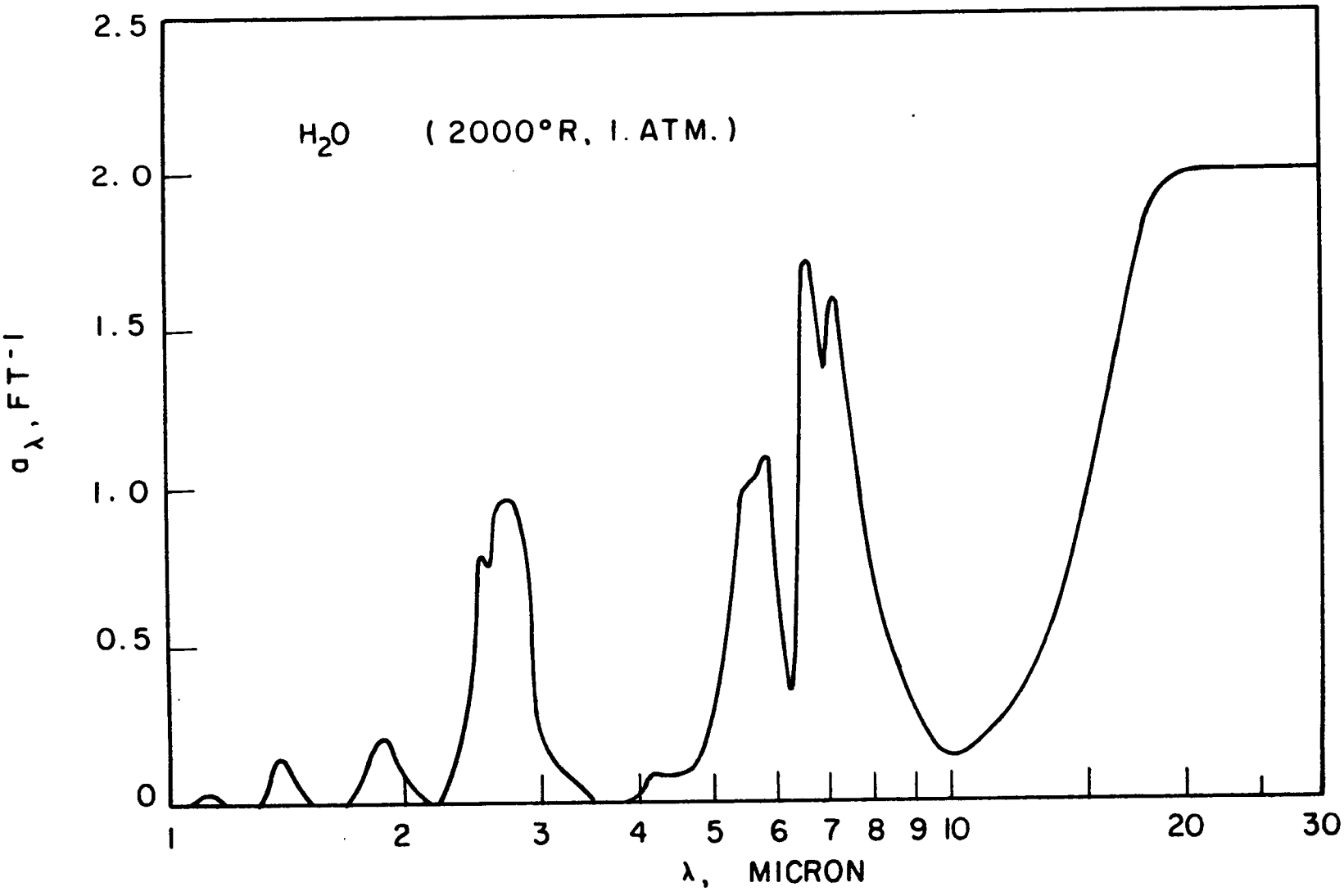


FIG. 26 INFRARED ABSORPTION SPECTRUM OF $H_2O$ AT 2000°R AND 1 ATM.

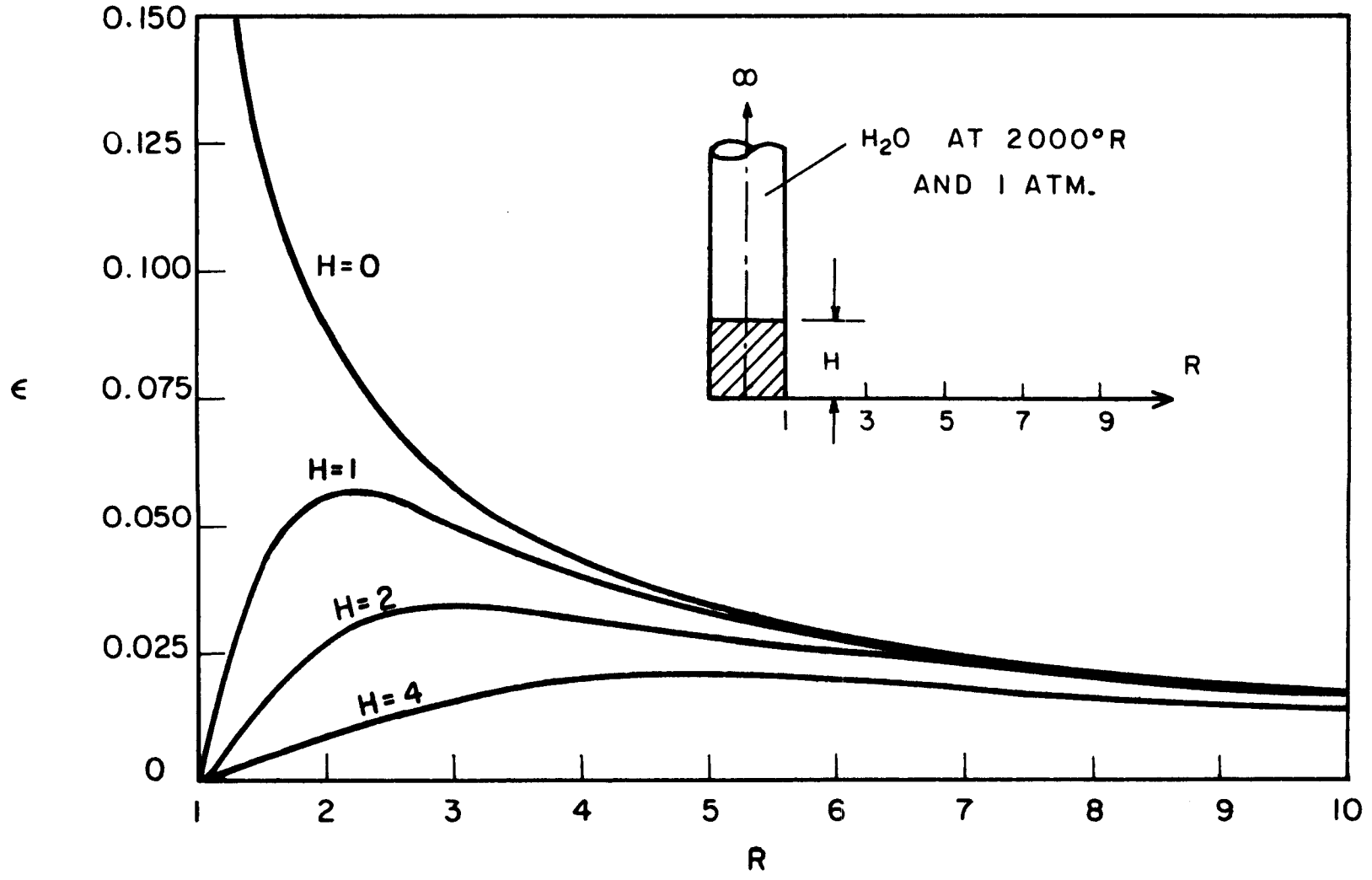


FIG. 27 APPARENT EMISSIVITIES IN THE BASE PLANE OF A SEMI-INFINITE CYLINDER OF WATER VAPOR AT 2000°R AND ONE ATMOSPHERIC PRESSURE

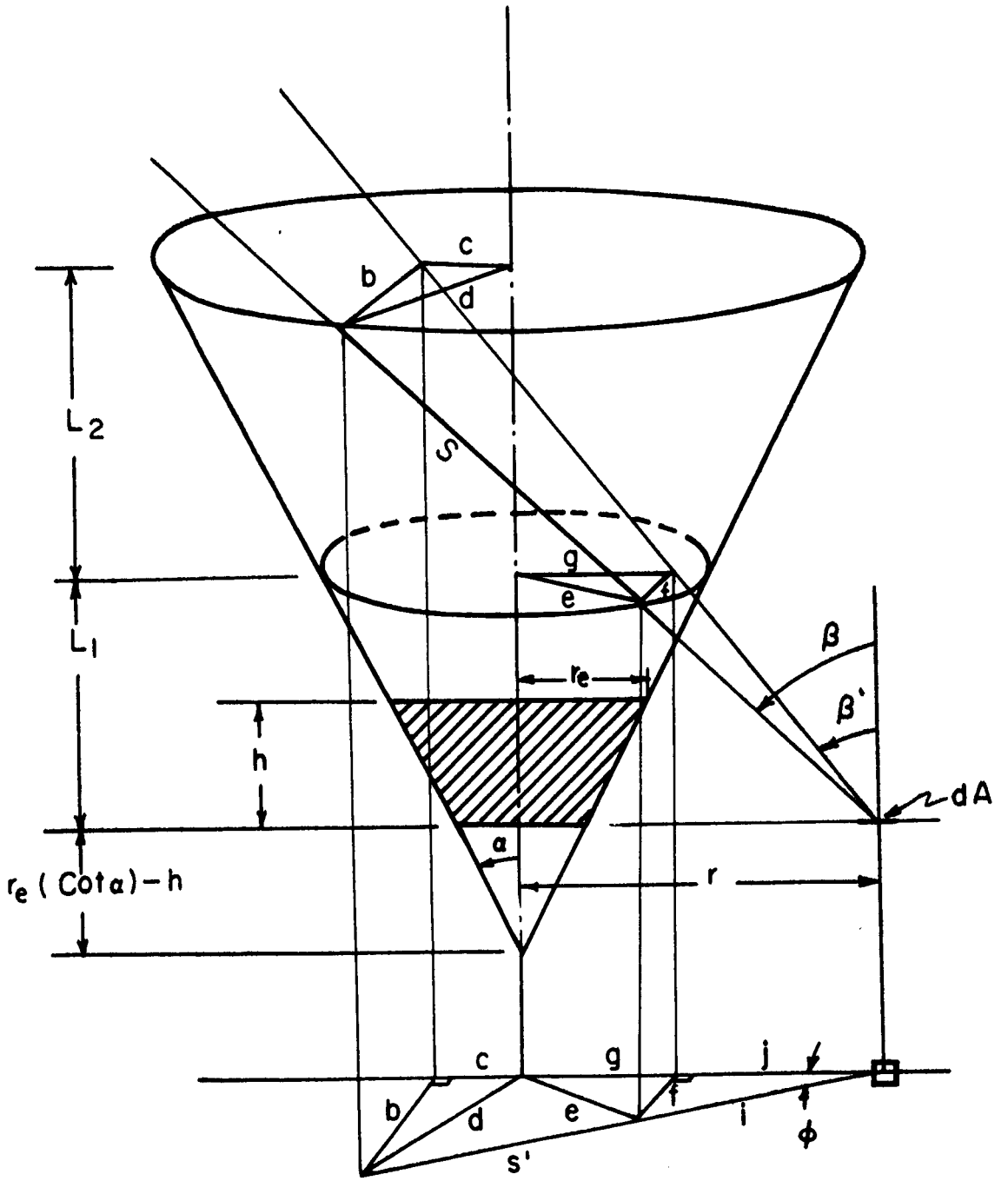


FIG. C-1 THE PATH LENTH THROUGH A CONICAL GAS BODY